JOURNAL OF SPACECRAFT AND ROCKETS

Options for a Nondedicated Mission to Test the Pioneer Anomaly

Andreas Rathke*
EADS Astrium GmbH, 88039 Friedrichshafen, Germany
and
Dario Izzo†
ESA, 2201 AZ Noordwijk, The Netherlands

The Doppler-tracking data of the Pioneer 10 and 11 spacecraft show an unmodeled constant acceleration in the direction of the inner solar system. Serious efforts have been undertaken to find a conventional explanation for this effect, all without success at the time of writing. Hence, the effect, commonly dubbed the Pioneer anomaly, is attracting considerable attention. Unfortunately, no other space mission has reached the long-term navigation accuracy to yield an independent test of the effect. To fill this gap, strategies are discussed for an experimental verification of the anomaly via an upcoming space mission. Emphasis is put on two plausible scenarios: nondedicated concepts employing either a planetary exploration mission to the outer solar system or a piggybacked microspacecraft to be launched from a mother spacecraft traveling to Saturn or Jupiter. The impact of a Pioneer anomaly test on the system and trajectory design for these two paradigms is analyzed. It is found that both paradigms are capable of verifying the Pioneer anomaly and determine its magnitude at 10% level. Moreover, the concepts can discriminate between the most plausible classes of models of the anomaly, a central force, a blueshift of the radio signal, and a draglike force. The necessary adaptions of the system and mission design do not impair the planetary exploration goals of the missions.

Nomenclature

$A_{S/C}$	=	cross-sectional area of the spacecraft, m^2
a_H	=	Hubble acceleration, m/s^2
$a_\odot$	=	acceleration due to solar radiation pressure, m/s^2
c	=	speed of light, $\approx 3 \times 10^8$ m/s
$\boldsymbol{e}_A$	=	unit vector normal to the area A
$\boldsymbol{e}_\odot$	=	unit vector pointing towards sun
F	=	force, N
f	=	generic tracking observable
g_0	=	gravitational acceleration at the Earth's surface, m/s^2
I	=	moment of inertia, $kg \cdot m^2$
I_{sp}	=	specific impulse, s
k	=	Boltzmann constant, J/K
$M_{S/C}$	=	spacecraft wet mass, kg
M_α	=	total mass of α particles produced by radioactive decay, kg
H_0	=	Hubble constant, km/s · Mpc
P_a	=	asymmetrically radiated power, W
P_{tot}	=	total radiated power, W
$P_\odot$	=	solar radiation constant 1367 WAU^2/m^2
R	=	universal gas constant, J/kg · K
r	=	heliocentric distance, m
r_p	=	radius of pericentre from planet P, km
$r_\oplus$	=	mean radius of Earth orbit, m
s	=	geocentric distance of spacecraft, km
s^*	=	deviation from nominal spacecraft trajectory, km
T	=	temperature, K
T_s	=	stagnation temperature, K
T_{tank}	=	temperature of fuel in tank, K
T_0	=	temperature at nominal emissivity, K
t	=	time, s
t_e	=	time of departure at Earth, modified Julian date (MJD)
t_p	=	time of arrival/swingby at planet, MJD
$t_\oplus$	=	orbital period of the Earth, s
V_P	=	heliocentric velocity of planet P, km/s
v_{in}	=	inbound asymptotic velocity, km/s
v_{out}	=	outbound asymptotic velocity, km/s
v_α	=	velocity of α particles, m/s
$v_\oplus$	=	mean heliocentric velocity of the Earth, km/s
$\alpha_\oplus$	=	longitude in geocentric ecliptic coordinate system, deg
α^*	=	deviation from nominal geocentric azimuth angle, deg
β	=	angle between Earth–spacecraft direction and direction of anomaly, deg
$\beta_\odot$	=	angle between sun–spacecraft direction and direction of anomaly, deg
$\beta_\oplus$	=	Earth–spacecraft–sun angle, deg
γ	=	flight angle (angle between velocity vector and local horizontal), deg
Δa	=	systematic uncertainty of acceleration a, m/s^2
Δf	=	uncertainty on the generic tracking observable, f
ΔM	=	mass of expelled propellant, kg
Δs	=	systematic uncertainty on the geocentric distance s, km
Δv	=	systematic uncertainty on the velocity v, km/s
ΔV	=	velocity increment, km/s
$\Delta\epsilon$	=	change of emissivity per angle
$\Delta\epsilon_{max}$	=	maximal change of emissivity
$\Delta\mu_\odot$	=	change of the effective reduced solar mass, km^3/s^2
ϵ_0	=	nominal emissivity per angle
η	=	specular reflectivity
θ	=	angle enclosed by $\boldsymbol{e}_A$ and $\boldsymbol{e}_\odot$, deg
κ	=	adiabatic exponent
μ_P	=	reduced mass of planet P, km^3/s^2
$\mu_\odot$	=	reduced solar mass, km^3/s^2
ρ	=	true heliocentric distance, km
σ	=	standard deviation
ϕ	=	mean anomaly of Earth orbit, deg
ψ	=	azimuth angle of cylinder coordinates, deg

Received 28 April 2005; revision received 10 October 2005; accepted for publication 15 November 2005.

*System Engineer, Department AED41; andreas.rathke@astrium.eads.net.
†Research Fellow, Advanced Concepts Team, European Space Research and Technology Center, Keplerlaan 1; dario.izzo@esa.int.

ω = rotational velocity of spacecraft, deg/s

Subscripts

track = tracking error
0 = at time $t = 0$, that is, beginning of measurement
$\parallel$ = parallel to Earth–spacecraft vector
$\perp$ = orthogonal to Earth–spacecraft vector
$\odot$ = solar
$\oplus$ = Earth/terrestrial

Superscript

$*$ = anomalous

I. Introduction

DOPPLER tracking data of the Pioneer 10 and 11 deep-space probes show a deviation between the orbit reconstruction of the spacecraft and their Doppler tracking signals.[1,2] This discrepancy, which has become known as the Pioneer anomaly, can correspond either to a small constant deceleration of the spacecraft of roughly 9×10^{-10} m/s^2 or to an anomalous blueshift of the radio signal at a rate of 6×10^{-9} Hz/s. Because no unambiguous conventional mechanism to explain the anomaly, such as an onboard force, has been identified, there is a growing number of studies that consider an explanation in terms of a novel physical effect.

In April 2004, the ESA invited the scientific community to participate in a call for themes for cosmic vision 2015–2025, to assist in developing future plans of the Cosmic Vision Programme of the ESA Directorate of Science. Among the 32 proposals received in the field of fundamental physics, five propose a space experiment to investigate the Pioneer anomaly. In its recommendation for the Cosmic Vision Programme, the Fundamental Physics Advisory Group of ESA considered these proposals as interesting for further investigation.[3] In view of the controversial discussion still surrounding the effect, on the one hand, and its high potential relevance for our understanding of the laws of physics, on the other hand, the FPAG recommended that ESA should study the possibility of investigating the putative anomaly onboard a nondedicated exploration mission.

Motivated by this important discussion, we provide a preliminary assessment of the capabilities of missions to the outer solar system to investigate the Pioneer anomaly. We identify two classes of mission that could well represent a future exploration mission. The first class is that of low-mass low-thrust orbiter missions to the outer planets. The second class is that of a heavy, nuclear-reactor powered spacecraft, as proposed earlier by NASA's Prometheus Program, to explore the giant planets. Within these two paradigms, we analyze missions to all planets from Jupiter outward and consider to what extent a verification and characterization of the Pioneer anomaly is possible.

The layout of our considerations is the following: We begin with a review of the Pioneer anomaly in Sec. II. After a description of the observed anomaly in the Pioneer tracking in Sec. II.A, we turn to the considerations that have been put forward to explain the anomaly in terms of systematics in Sec. II.B. In Sec. II.C, we review approaches to explain the anomaly as a novel physical effect. This review leads us to the formulation of the experimental requirements that a mission to test the Pioneer anomaly has to fulfill in Sec. II.D. In Sec. II.E, we discuss the navigational accuracy of past and present deep-space missions and explain why none of these mission is likely to decide the issue if the Pioneer anomaly is indeed of physical significance. In Sec. III, we turn to the discussion of non-dedicated mission concepts for a test of the Pioneer anomaly. We start by discussing the major design drivers for missions to the outer solar system in Sec. III.A. Then in Secs. III.B and III.C, we give an overview of the two scenarios that we consider. IN Sec. IV, we discuss in detail the necessary design considerations to reduce the systematic accelerations onboard a deep-space probe to a tolerable amount for a test of the Pioneer anomaly. In particular, aspects of thrust history uncertainties (Sec. IV.A), fuel leaks and outgassing (Sec. IV.B), thermal radiation (Sec. IV.C), the radio-beam reaction force (Sec. IV.D), and solar radiation pressure (Sec. IV.E) are addressed. In Sec. IV.F, the estimated error budget is summarized, and in Sec. IV.G, the necessary modifications in the spacecraft design to fulfill the test requirements are summarized. The second major topic is the development of a measurement strategy for the test in Sec. V. In Sec. V.A we investigate the instrumentation options for an verification of the anomaly. It is found that the experiment will have to rely on radio tracking. Consequently, we review the available radio-tracking methods in Sec. V.B. This is followed by a discussion in Sec. V.C of the relevant tracking observable. In Sec. V.D, the radio-tracking performance of the two mission paradigms is estimated. Based on the design and mission requirements obtained, the space of trajectory options is explored in Sec. VI. This is done separately for the two mission paradigms in Secs. VI.A and VI.B. The conclusions of our analysis are summarized in Sec. VII.

II. Pioneer Anomaly

A. Tracking-Data Anomaly

The Pioneer 10 and 11 spacecraft, launched on 2 March 1972 and 5 April 1973, respectively, were the first to explore the outer solar system. (See Lasher and Dyer[4] for an overview of the Pioneer 10 and 11 missions.) Since its Jupiter gravity assist on 4 December 1973, Pioneer 10 is on a hyperbolic coast. In the heliocentric J2000 reference frame, the ascending node of the asymptote was (and has since remained) -3.4 deg; the inclination of the orbit is 26.2 deg. Pioneer 11 used a Saturn swingby on 1 September 1979 to reach a hyperbola with an asymptotic ascending node of 35.6 deg and an inclination of 9.5 deg. The orbit determination for both craft relied entirely on Doppler tracking.

Before the Jupiter swingby, the orbit reconstruction for Pioneer 10 indicated an unmodeled deceleration of the order of 10^{-9} m/s^2, as first reported by Null.[5] This effect was, at that time, attributed to onboard generated systematics, that is, unmodeled behaviors of the spacecraft systems), in particular, to fuel leaks. However, an unmodeled deceleration also remained during the hyperbolic coast, although the number of attitude-control maneuvers was reduced to approximately one every five months. Hence, fuel leakage, triggered by thruster activity, could no longer be considered as an explanation. Even more surprising, the Doppler tracking of Pioneer 11 also shows an unmodeled deceleration of a similar magnitude.

The anomaly on both probes has been subject to three independent analyses that used different orbit determination programs.[1,2,6] The conclusion of all of these investigations was that an anomalous Doppler blueshift is present in the tracking data of both craft and that the magnitude of the blueshift is approximately 1.1×10^{-8} Hz/s, corresponding to an apparent deceleration of the spacecraft of approximately 9×10^{-10} m/s^2. Note that from the Doppler data alone it is not possible to distinguish between an anomalous frequency shift of the radio signal; in conventional terms this could also indicate a drift of the Deep Space Network clocks and a real deceleration of the spacecraft (cf. Sec. V.C). The observational data and the subsequent analysis are described in detail in the work of Anderson et al.[2] and Markwardt.[6] The results of these different analyses show a discrepancy at a level of approximately 5% of the inferred deceleration. Unfortunately, none of the analyses performed made use of the entire data set available.

The quality of the data is best judged from the plot of the Pioneer 10 anomalous acceleration as determined by the CHASMP software (developed by The Aerospace Corporation) and reported by Anderson et al.[2] (Ref. 2, Fig. 9). Whereas it is quite obvious that the data show the existence of an anomalous acceleration, it is also obvious that the variation of the measured anomaly due to systematics is too big to evaluate the first derivative of the anomaly. This noise is reflected in the large overall error for the value of the anomaly given by Anderson et al.,[2] $\Delta a^* = 1.33 \times 10^{-10}$ m/s^2. Nevertheless, the deviation from the nominal Doppler shift is highly significant: The orbit reconstruction of Pioneer 10 is incompatible with the nominal orbit at 6σ level.[7]

B. Systematics?

Many attempts[8–16] have been made to interpret the anomaly as an effect of onboard systematics ranging from fuel leakage to heat radiating from the spacecraft. Unfortunately, the conclusions of the various studies are far from unanimous. In the work of Anderson et al.[2] it is concluded that none of the effects considered is likely to have caused the anomaly. They argue that a heat-generated anomaly would be mainly due to the heat of the radioisotope thermoelectric generators (RTGs) and that this can be excluded because the heat decay from the plutonium half-life of 87.7 years would have shown up as a decrease of the deceleration in the longest analysed data interval for Pioneer 10, ranging from January 1987 to July 1998.

They note that gas leaks can be excluded as the cause of the anomalous deceleration, under the sole assumption that the amount of fuel leakage is uncorrelated between Pioneer 10 and 11. However, because both spacecraft designs are identical, two identical gas leaks can, ultimately, not be excluded.

At the current stage of investigation, it is not even clear if one should attribute the anomaly to a conventional effect or consider explanations rooted in new physical phenomena. A complete examination of the full archive of Doppler data is certainly needed. Nevertheless, even with this enhanced knowledge it seems highly doubtful that the issue can be decided because there exist considerable uncertainties in the modeling of forces generated onboard Pioneer 10 and 11. In view of the necessity for an improved evaluation of the Doppler data, the authors feel obliged to express their unease about the discrepancies between the results obtained with the different orbit-determination programs. In particular, note that the disagreement between the three analyses is bigger that their nominal errors.

C. New Physics?

The inability to explain the Pioneer anomaly with conventional physics has contributed to the growing discussion about its origin. The possibility that it could come from a new physical effect is now being seriously considered. In particular, the coincidence in magnitude of the Pioneer anomaly and the Hubble acceleration has lead to the suggestion that the Pioneer anomaly could be related to the cosmological expansion.

Although the Pioneer anomaly is an effect at the border of what is detectable with radiometric tracking of a deep-space probe, it is huge in physical terms. The anomaly exceeds by five orders of magnitude the corrections to Newtonian motion predicted by general relativity [at 50 astronomical units (AU) solar distance]. (Note that the leading-order relativistic correction is $\sim F_N v^2/c^2$, where F_N is the Newtonian gravitational force; compare, for example, Montenbruck and Gill,[17] pp. 110ff.) Hence, if the effect is not due to systematics, it would have a considerable impact on our models of fundamental forces, regardless of whether the anomaly was due to a deceleration of the spacecraft or a blueshift of the radio signal.

One of the obstacles to an explanation of the Pioneer anomaly in terms of new physics is that a modification of gravitation, large enough to explain the Pioneer anomaly, easily runs into contradiction to the planetary ephemerides. This becomes particularly clear if one considers the orbit of Neptune. At 30 AU, the Pioneer anomaly is visible in the Doppler data of both Pioneer 10 and 11. The influence of an additional radial acceleration of $a^* = 9 \times 10^{-10}$ m/s^2 on Neptune is conveniently parameterized in a change of the effective reduced solar mass $\mu_\odot$ felt by the planet.[18] The resulting value, $\Delta\mu_\odot = a^* r^2 = 1.4 \times 10^{-4}\,\mu_\odot$, is nearly two orders of magnitude beyond the current observational constraint of $\Delta\mu_\odot = (-1.9 \pm 1.8) \times 10^{-6}\,\mu_\odot$ (Ref. 19). Similarly, the Pioneer 11 data contradict the Uranus ephemerides by more than one order of magnitude. Thus, the Pioneer anomaly can hardly be ascribed to a gravitational force because this would indicate a considerable violation of the weak equivalence principle. In particular, planetary constraints rule out an explanation in terms of a long-range Yukawa force (see Refs. 2 and 20).

In the first paper discussing the Pioneer anomaly, it was noted that the magnitude of the effect coincides with the Hubble acceleration and with the so-called modified Newtonian dynamics (MOND) parameter.[1] Subsequently there have been several attempts to associate the Pioneer anomaly both with the cosmic expansion and with the MOND model. The Hubble acceleration a_H is formed by converting the Hubble expansion rate H_0 (Ref. 21), to an acceleration by multiplying it by the speed of light, $a_H \equiv cH_0 = (6.9 \pm 0.7) \times 10^{-10}$ m/s^2. [The Hubble acceleration is by no means an artificial construct but is related to actual observables. For instance, it describes the lowest-order correction from the cosmic expansion to the length of light rays from a past event to a present-day observer $d = c\Delta t + (a_H/2)(\Delta t)^2$.] Attempts to connect the Pioneer anomaly with the cosmic expansion consider both possibilities: that the Pioneer anomaly only affects light propagation,[22–27] or that it causes a real deceleration of the spacecraft.[28–29] However, the predominant opinion, starting with the work of Einstein and Straus,[30] is that cosmic dynamics has far too little influence to be visible in any physical processes in the solar system. The case has recently been reviewed, confirming the common opinion.[31] Other problems with this approach are the apparent violation of the weak equivalence principle associated with the Pioneer anomaly and the opposite signs of the cosmic expansion and of the Pioneer anomaly.

MOND is a long-distance modification of Newtonian gravity that successfully explains the dynamics on galactic scales without invoking dark matter (see Ref. 32 and see Sanders and McGaugh[33] for a review). The MOND parameter $(1.2 \pm 0.3) \times 10^{-10}$ m/s^2 gives the acceleration scale at which the gravitational force changes from the Newtonian law to the MOND law that predicts stronger gravitational attraction. Whereas MOND is consistent and successful as a nonrelativistic theory, its relativistic generalizations remain unsatisfactory because they require a fixed background structure or even have acausal features.[34] The Pioneer anomaly can be connected with MOND if one assumes that the transition between the Newtonian and MOND regimes can be approximated by a Taylor series around the Newtonian potential and that the MOND parameter sets the magnitude of the first term in this Taylor expansion (see Ref. 34). Similarly, the flatness of galactic rotation curves and the Pioneer anomaly could be connected in a gravitational theory based on a nonsymmetric metric.[35]

To circumvent the constraints from planetary ephemerides, momentum-dependent nonlocal modifications of general relativity have also been considered.[36–38] Whereas the original idea is rather vague, a more elaborate model[37,38] faces several problems. Jaekel and Reynaud,[37] introduced two different momentum-dependent **Q5** gravitational constants for the trace and the conformal sector of the Einstein equations. Such running couplings lead to a violation of the Bianchi identities unless one resorts to a nonlocal reformulation of the Einstein–Hilbert action (see Refs. 39 and 40). Even then, causality of the resulting physical laws needs careful consideration. Even worse, this modification results in an unstable dipole-ghost (cf., Smilga[41]). It seems hard to conceive that the combination of instability and fine-tuning between the scalar and conformal sectors can result in a viable model.

There are several other works pursuing even more unusual lines of explanation. See the papers by Anderson et al.[2] and by Bertolami and Paramos[42] for reviews of some of the proposed explanations of the Pioneer anomaly that rely on more exotic physics. The models considering a blueshift of the radio signal are reviewed by Defrère and Rathke.[43] To now, all of the models to explain the Pioneer anomaly in terms of new physics still have to be considered as incomplete. In view of the current rapid development of the field, however, one might expect considerable progress in the next few years.

D. Experimental Requirements for a New Test

From the analysis of the Pioneer tracking data and the theoretical approaches to their explanation, one can deduce the requirements for a new test of the anomaly. For a verification of the anomaly, one would need a spacecraft with an acceleration systematics below the magnitude of the anomaly. A long-lasting ballistic phase in the trajectory is mandatory so that the search for the anomaly is not overwhelmed by thruster activity. Furthermore, because it is

unknown if the anomaly is generated by a force or by an anomalous blueshift of the radio signal, the experiment has to be sensitive to both possibilities.

These generic requirements may be amended by model-dependent requirements stemming from the theoretical analysis of the anomaly. If the anomaly is caused by a modification of the gravitational laws, it would require a violation of the weak equivalence principle. The most plausible realization of this would be via a momentum dependence of the gravitational attraction. To be sensitive to such an effect, one requires a high radial velocity of the spacecraft with respect to the sun. This corresponds to a highly eccentric, preferably hyperbolic, trajectory of the spacecraft.

An explicit dependence of the anomalous force on the position of the spacecraft within the solar system is highly improbable. This follows from the observation that the anomalies on both Pioneer probes do not change significantly with the position of the spacecraft along their orbits. (A small change cannot be excluded due to the large error margin of the data): Also the trajectories of the two Pioneers are heading away from the sun in approximately opposite directions and at considerably different inclinations, thus, making it possible to conclude that if such a dependence exists, then it has to be so small as to be undetectable from study of the Pioneer data.

One might also envisage that the spin of the spacecraft has an influence on the magnitude of the anomalous force. (See Refs. 14–16, which describe an unsuccessful attempt to locate the origin of the anomaly in the rotation of the Pioneer probes.) Such a dependence may be reasonably excluded. The rotational speed of the Pioneer 10 spacecraft was 4.5–4.2 rpm; that of Pioneer 11 was about 7.3–7.2 rpm. When a power-law dependence of the anomalous acceleration a on the rotational velocities of the spacecraft ω is assumed, $a^* = \text{const}\ \omega^x$, the exponent being constrained by the error margin of the anomalous acceleration to $|x| < 0.7$. Thus, in particular, a linear dependence of the anomalous acceleration on the rotational velocity, and a linear dependence of the anomalous acceleration on the rotational energy of the spacecraft, $E_{\text{rot}} = I\omega^2/2$ with I being the moment of inertia along the spin axis, is ruled out. Hence, a dependence of the anomaly on the rotational parameters of the spacecraft seems rather unlikely and in the following study, no requirements on the rotational velocity will be considered.

One might want to augment the preceding requirements for a verification of the anomaly by requirements that would allow a further characterization of the anomaly. In particular, it would be of great interest to test if the anomaly is caused by a force gravitational type, that is, new physics, or nongravitational type, systematics. Of course, an improved acceleration sensitivity of the spacecraft might allow a determination of the force law that generates the anomaly, for example, its gradient.

Before we turn to the implementation of high-acceleration sensitivity in the design of an exploration spacecraft in Sec. IV, we consider the performance of several past, present, and upcoming deep-space missions for a test of the Pioneer anomaly.

E. Other Spacecraft

It stands to reason that if the anomaly detected in the tracking data of the Pioneers, were due to some unknown fundamental physical phenomenon the anomaly should be observed in the data from other missions as well. For various reasons, up to now no other mission has reached the long-term navigational accuracy of the Pioneer 10 and 11 spacecraft. Here we identify the design characteristics that led to the lower navigational performance of the other past missions to the outer solar system and discuss the performance expectations for current missions, which have not been designed with a test of the Pioneer anomaly as a (secondary) mission goal.

This issue has already been analyzed in detail for the Voyager spacecraft and for Galileo and Ulysses.[2] The basic conclusion is that the three-axis stabilization system of the Voyager probes performs so many attitude-control maneuvers that it is impossible to detect the anomalous acceleration on these spacecraft. For Galileo and Ulysses, the large systematic errors due to solar radiation pressure and malfunctions of part of the attitude-control systems prohibited any reliable result.

Also the Cassini tracking does not yield results of the necessary precision because the spacecraft is three-axis stabilized.[7] Furthermore, thermal radiation from the RTGs causes a large acceleration bias, the magnitude of which is not well determined. The large bias originates from the placement of the RTGs close to the spacecraft bus. The thermal control of the propulsion module subsystem is accomplished by collecting thermal radiation from the RTGs in a cavity covered with insulating blankets.[44] The radiation geometry of the cavity is complicated and leads to a large uncertainty in the acceleration bias due to RTG heat.

Among the current missions, ESA's Rosetta mission[45] to the comet Churymov–Gerasimenko has a trajectory to the outer solar system that would seem suited for verifying the Pioneer anomaly. The Rosetta trajectory has a long elliptical coast arc from July 2011 to January 2014, during which the distance from the sun will increase from 4.5 to 5.4 AU. Unfortunately, the system design and operations of the spacecraft will not allow a successful test of the Pioneer anomaly. During the coast arc, the Rosetta craft will enter a so-called hibernation mode, when the power generated by the solar arrays drops below a certain value. In this mode, the spacecraft will be spin-stabilized with a rotational velocity of approximately 1 rpm. Most onboard instruments, including the attitude-control and radio-transmission systems, will be switched off. Unfortunately, during the hibernation no tracking can be performed; hence, the presence of a force can only be inferred from the trajectory evolution between the entry and exit of hibernation. The large 68-m^2 solar arrays on the craft will cause an acceleration bias of approximately 10^{-8} m/s^2, one order of magnitude larger than the Pioneer anomaly. Because the orientation of the solar arrays during the hibernation phase is not actively maintained, a large uncertainty in the solar radiation force on the spacecraft, $\sim 10^{-9}$ m/s^2, will result. Hence, both the large unknown acceleration systematics and the lack of regular tracking passes will prohibit a test of the anomaly with Rosetta.

Close to the class of exploration missions discussed in this work, is NASA's New Horizons mission.[46] The destination of this mission is Pluto, and the launch is scheduled for 2006. Also for this mission no test of the Pioneer anomaly is foreseen. On the contrary, the mission baseline foresees that the spacecraft will be in a spin-stabilized mode with little onboard activity and infrequent tracking passes during most of the journey, similar to Rosetta. In contrast to Rosetta, this mode is not required by power constraints and was mainly chosen to increase component lifetime and reduce operation costs. Hence, an enhanced tracking of the mission for a test of the Pioneer anomaly would be possible in principle. However, doubts remain that a sufficient knowledge of onboard acceleration biases can be achieved to render such a test reliable. The system design of the mission is far from ideal for a test of the Pioneer anomaly. The RTG of New Horizons is directly attached to the spacecraft bus. This design will lead to a considerable backscattering of RTG heat from the back of the antenna, causing a large acceleration bias, most likely one order of magnitude larger than the Pioneer anomaly, along the spin axis of the spacecraft. The determination of this acceleration bias to sufficient accuracy to disentangle it from a putative anomaly would most likely require a purpose-made high-accuracy thermal radiation model. The difficulties in the determination of the bias are aggravated by a possible degradation of the surface properties of the RTG and the back of the antenna during the flight. (See Sec. IV.C for a general discussion of these issues.) Hence, even with an enhanced tracking coverage, the system design of the New Horizons spacecraft will be a considerable obstacle for any attempt to verify the Pioneer anomaly with this mission.

The inability of various missions to achieve a long-term navigational accuracy comparable to that of Pioneer 10 and 11 demonstrates that both the system design and the trajectory design will need careful consideration to accomplish a test of the Pioneer anomaly. From the failures of Galileo and Ulysses and the deficits of New Horizons, it is clear that simply requiring a spin stabilized spacecraft on a mission to the outer solar system will not be sufficient. Detailed considerations are necessary to reduce the acceleration systematics on the test spacecraft to a sufficient level. In the next section, we turn to the system design challenges posed by a Pioneer anomaly test and

we present design solutions to reduce the acceleration uncertainty that are feasible in nondedicated scenarios.

III. Nondedicated Mission Concepts

A. Capabilities of Exploration Missions

Dedicated missions to verify and characterize the Pioneer anomaly are presently being intensively considered, and at least two promising concepts have been identified. The more conventional one is that of a highly symmetric spacecraft with strong suppression systematic accelerations.[7,47,48] The acceleration sensitivity is expected to reach 10^{-11} m/s^2. The performance of a Pioneer anomaly test is even further improved in the second concept.[49–51] Here a spacecraft with small acceleration systematics is envisaged to release a small subsatellite of reflective-sphere type. The subsatellite is completely passive and is practically free of any systematic accelerations. It is tracked from the mothercraft by laser ranging or radar. The interspacecraft tracking signal is combined with radio tracking of the mothercraft from the Earth to monitor any deviation of the subsatellite from geodesic motion. The expected acceleration sensitivity of this setup is 10^{-12} m/s^2.

A nondedicated mission is not expected to reach the full performance of the dedicated concepts. However, it has the major advantage of coming at considerably reduced costs provided a suitable mission can be identified to host the experiment without interfering with the primary mission goals. Exploration missions to the outer solar system offer such an opportunity to test the Pioneer anomaly. Missions to Uranus, Neptune, or Pluto would most naturally feature, at a certain point, a Jupiter gravity assist followed by a hyperbolic coast arc. This coast phase lends itself to precision tracking of the spacecraft trajectory, which can be analyzed to detect anomalous accelerations. The major design drivers for such a mission would, however, be the planetary exploration goals. Hence, a design such as the symmetric spacecraft described by Anderson et al.[48] would be excluded because of payload requirements, for example, field of view, and the need to accommodate a propulsion module capable of achieving a capture into the orbit of the target planet. The use of a special experimental payload able to test the Pioneer anomaly would most probably also be excluded because of mass constraints. However, even under these conditions, an investigation of the Pioneer anomaly is still attainable. Although additional requirements on the spacecraft design are imposed, these requirements can be fulfilled with no additional mass, little-to-no impact on the other observational program of the satellite, and no additional risks.

We will first consider a class of low-mass, low-thrust missions inspired by the study of a Pluto orbiter probe (POP)[52,53] and demonstrate the feasibility of a Pioneer anomaly test on such a mission. We then consider large spacecraft with electric propulsion powered by nuclear reactors such as those sometimes envisaged to explore the moons of the giant planets Jupiter and Saturn. One such spacecraft was until recently considered by NASA under the name of Jupiter Icy Moons Orbiter (JIMO). Whereas the large amount of heat radiated from the nuclear reactor on the craft would prohibit a test of the Pioneer anomaly on the main spacecraft, this class of missions could accommodate a small daughter spacecraft of less than 200-kg mass (compared with the 1500 kg of payload envisaged for JIMO). This spacecraft could then be jettisoned during the approach of the mothercraft to the target planet and could use the planet for a powered gravity assist to achieve a ballistic hyperbolic trajectory. The Pioneer anomaly test would then be performed by the daughter spacecraft.

B. POP Spacecraft

POP is an advanced spacecraft designed within the Advanced Concepts Team of ESA[52–55] that is capable of putting a 20-kg payload into a low-altitude Pluto orbit. The preliminary design has a dry mass of 516 kg and a wet mass of 837 kg. The spacecraft is powered by four RTGs. The original mission profile envisages a launch in 2016 and arrival at Pluto after 18 years of travel time, including a Jupiter gravity assist in 2018. A suitable launch vehicle would be an Ariane 5 Initiative 2010. The preliminary design of POP consists of a cylindrical bus, of 1.85 m length and 1.2 m diameter. The 2.5-m-diam Ka-band antenna is mounted on one end of the main structure. The four general-purpose heat-source (GPHS) RTGs are placed at the other end of the main structure, inclined 45 deg to the symmetry axis of the craft. The four QinetiQ T5 main engines are also placed at this end of the main structure. Next to the main engines in the main structure is the propellant tank accommodating 270 kg of xenon propellant. POP is a good example of what an advanced spacecraft to the outer solar system may look like, and we, therefore, take it as a paradigm for this kind of mission. Table 1 gives the key figures of POP that are relevant for our reasoning.

Table 1 Relevant spacecraft data for two mission paradigms

Parameter	POP	Microspacecraft
Wet mass during coast, kg	750	150
Electric power, W	1000	100
RTG heat, W	10000	1000
Maximal radio-transmission power, W	50	10
Antenna diameter, m	2.5	1.5

C. Piggyback Microspacecraft

In the framework of NASA's Prometheus Program, JIMO was proposed by NASA as the first mission to demonstrate the capabilities of electric propulsion powered by a nuclear reactor. The mission, recently canceled due to recent NASA priorities, is still a plausible architecture for other future exploration missions. Because of its high payload capabilities, a JIMO type of mission could carry a microspacecraft to test the Pioneer anomaly. The spacecraft would be jettisoned at some point on the trajectory and put into hyperbolic heliocentric trajectory via a planetary gravity assist. This would allow the spacecraft to perform a Pioneer anomaly test after its swingby.

A possible baseline design for the piggyback spacecraft, resulting from the design driver of reducing onboard-generated systematics, is that of a spin-stabilized craft. A preliminary mass estimate and power budget can be based on the results of ESA's study of an Interstellar Heliopause Probe,[56] which has a similar baseline. The result yields a mass of 150 kg. The spacecraft would use ion thrusters, for example, hollow-cathode thrusters, for attitude control and carry only a minimal scientific payload. Because only a small data rate would be required, a 1.5-m high-gain antenna would be sufficient even in the outer solar system. The required 80 W of power to operate the payload, the communication subsystem, and the attitude and onboard control system would be provided by two RTGs weighing 12.5 kg each. Heat pipes from the RTGs to the main structure of the spacecraft would be used for thermal control.

In addition, a chemical propulsion module would be necessary to provide a moderate ΔV before and during the swingby. This propulsion stage would be jettisoned after the swingby, to eliminate the danger that residual fuel might leak from the module and spoil the Pioneer anomaly test. The dry mass of the module is estimated to be 16 kg. A detailed design is beyond the scope of this paper. We apply a 20% mass margin and a 20% margin on the required power. Accelerations due to onboard generated systematic errors are inversely proportional to the mass of the spacecraft. Hence, for the calculation of the error budget, the conservative estimate will arise from assuming the lower mass for the spacecraft but the higher power consumption. The relevant parameters considered for the piggyback microspacecraft are summarized in Table 1.

IV. Spacecraft Design

From our review of missions to the outer solar system, we saw that a major obstacle for a test of the Pioneer anomaly is a lack of knowledge about the onboard-generated forces, which are typically one order of magnitude larger than the Pioneer anomaly (cf. Longuski et al.[57]). The aim of this section is to demonstrate that it is possible to reduce the overall onboard-generated systematics to less than 10^{10} m/s^2, that is, less than 10% of the Pioneer anomaly, by adopting, at the early design phase, some spacecraft design expedients that do not spoil the planetary-science mission objectives. We

review the major possible sources of systematics and discuss how to reduce them to an acceptable level by a careful system design. Emphasis will be put on proof of concept by analytical considerations that facilitate physical insight into the proposed methods.

A. Thrust History Uncertainties

A precise knowledge of the thrust history of the spacecraft is necessary if we want to be able to see small forces acting on the spacecraft.[57] However, the thrust level of chemical or cold-gas control thrusters varies considerably from firing to firing. In addition, the firing of a thruster is usually followed by a considerable nonpropulsive outflow of propellant, which generates accelerations easily exceeding the magnitude of the Pioneer anomalous acceleration (Anderson et al.[2]). A more precise thrust history becomes available if ion engines are used for the control of the spacecraft. In addition, electric-propulsion systems generate considerably smaller forces than nonpropulsive fuel outflow (Sec. IV.B).

A more efficient solution is to reduce the number of attitude-control maneuvers. This is achieved by spin stabilization of the satellite. For the piggyback microspacecraft paradigm, this poses no problems, and it is convenient to choose a relatively high rotational velocity to guarantee the highest possible stability against disturbances. For the POP paradigm, spin stabilization seems to be in contradiction to the requirements of planetary science; because the instruments for the latter require high-pointing accuracy, pointing stability and slew rate capabilities are not provided by a spin-stabilized spacecraft. In reality, the requirements of a Pioneer anomaly test and planetary science are not in contradiction because the different objectives have to be fulfilled in different parts of the mission. Hence, the spacecraft can be in spin-stabilized mode during the coast phase, which will be used for the search for new forces, and change to three-axis stabilized mode when approaching its final destination. Also, for any gravity assist, three-axis stabilized control is desirable because it allows for a more precise control of the nominal swingby trajectory. The spinup before and spindown after the coast, in which the anomaly is tested, will be performed in deep space, where few external disturbances act on the spacecraft. Hence the spinup and spindown can be conducted over a long time span and will only consume a negligible amount of propellant (Izzo et al.[55]). Furthermore, no additional attitude acquisition hardware will be necessary. Thanks to the low-disturbance level in deep space, the rotational velocity of the satellite can be very low, $\sim$0.01 rpm, and the star trackers for the three-axis stabilised mode would still be sufficient for attitude acquisition. Indeed, the coast in spin-stabilized mode might even save mass because it reduces the operating time of the momentum/reaction wheels or gyros and, hence, reduces the required level of redundancy.

B. Fuel Leaks and Outgassing

A fuel leak from the attitude control system presents one of the best candidates for a conventional explanation of the Pioneer anomaly. Unfortunately, even in a new mission, it would be difficult to entirely eliminate the possibility of fuel leaks caused by a malfunctioning valve. The force F generated by a mass flow rate $\dot{m}$ is given by (Longuski et al.[57])

$$F = \dot{m}\sqrt{2RT_s(1+\kappa)/\kappa}$$

For chemical propellant systems, the stagnation pressure corresponds to the temperature in the tank, $T_s = T_{\text{tank}}$. Requiring that the maximal additional acceleration generated by propellant leakage should not exceed 10^{-11} m/s^2, that is, it remains two orders of magnitude below than the anomaly, then the maximally allowed forces are $F \lesssim 7.5 \times 10^{-9}$ N for the POP scenario and $F \lesssim 1 \times 10^{-9}$ N for the microspacecraft. The corresponding mass flow rates allowed would, therefore, be less than 5 g/year, assuming realistic tank temperatures higher than 100 K. This requirement is far too demanding for a typical chemical attitude-control system (Longuski and König[57]).

The problem of fuel leakage becomes more manageable for electric-propulsion systems that do not rely on high tank pressures to generate additional thrust. The propellant gas passes from the high-pressure tank at $\sim$150 bar and $\sim$300 K, through a central pressure regulator, before it is distributed to the engines at low pressure, $\sim$2 bar. A redundant layout of the pressure regulator would, thus, considerably reduce the risk of leakage by a valve failure. The internal leakage rate of a central pressure regulator in an electric-engine piping is typically (assuming xenon as a fuel without loss of generality) $\sim 10^{-8}$ lbar/s, and the external leakage is approximately 10^{-12} lbar/s. From these numbers, it is clear that, although external leakage is sufficiently under control for the purpose of a Pioneer anomaly test, it is necessary to further reduce internal leakage. This can be achieved by placing a small reservoir with a low-pressure valve after the central regulator. For the low-pressure valve, an even smaller internal leakage is attainable, while the reservoir accommodates the gas leaking through the regulator until the next thruster firing, so that pressure buildup infront of the low-pressure valve stays within its operational range. Hence, the use of electric propulsion as an attitude-control system alleviates the problem of fuel leaks, and one of the major candidates of systematics on the Pioneer probes can be eliminated, allowing us to assume $\Delta a_{\text{leak}} = 10^{-11}$ m/s^2 for both mission concepts under consideration. **Q9**

Outgassing from the main structure of the spacecraft will, in general, not play a big role in the error budget. This is mainly because the probe will already have traveled for a considerable time before the test of the Pioneer anomaly will be performed. Nearly all outgassing will have taken place when the probe was closer to the sun. A more important source of outgassing are the RTGs of the spacecraft. In general, the α-decay reaction in RTGs produces helium, which will evaporate from the spacecraft. The decay of 1 kg of ^{238}Pu produces approximately 4.2×10^{-12} kg/s of helium. Assuming an efficiency of 40 W/kg for the generation of electrical power, for example, 38.3 W/kg for the GPHS RTG used on Cassini, we obtain a helium flow rate per generated watt of electric power of $\dot{M}_\alpha/P = 1.1 \times 10^{-13}$ kg/W. Furthermore, it is reasonable to assume that the helium has reached thermal equilibrium before it flows out of the RTGs. (Actually, the helium plays an important role for thermal conduction in the RTG. We are grateful to M. M. Nieto for this information.) Then its average velocity is given by $v_\alpha = \sqrt{(3kT/m_\alpha)}$, where m_α is the mass of a helium atom and the temperature of the RTG will typically be about $T = 500$ K. Hence, the outstream velocity of the helium will be $v_\alpha = 1.7 \times 10^3$ m/s. Assuming that all helium flows out unidirectionally, and taking into account the power and mass values given in Table 1, we may work out the magnitude of the acceleration for the two spacecraft designs. In particular, for missions that have a nuclear electric-propulsion system, the expulsion of helium can make an important contribution, and its recoil effect on the spacecraft needs to be taken into consideration. This is done most easily by placing the pressure relief valves of the RTGs in a direction so that no net force results along the spacecraft's spin axis. The measure is particularly convenient because it does not require any modification of the RTG design. We assume that the uncertainty in the acceleration due to helium outgassing can be constrained to 2% of its worst case value, which corresponds to a placement of the valve perpendicular to the spin axis with a precision of 1 deg. For the planetary exploration missions, this results into an uncertainty of $\sim 4.2 \times 10^{-12}$ m/s^2, and for the piggyback concept, we find an uncertainty of $\sim 2.1 \times 10^{-12}$ m/s^2. **Q10**

C. Heat

Heat is produced and radiated from the spacecraft at various points. The dispersion of heat, necessary to maintain the thermal equilibrium in the spacecraft, produces a net force on the spacecraft of $F = P_a/c = 3 \times 10^{-9}$ N/W of nonisotropically radiated heat.

The heat generated in the main structure of the spacecraft will, in general, be of the order of a few hundred watts. Assuming the advocated spin stabilization of the craft, the thermal radiation perpendicular to the spin axis of the satellite will average out over one rotation. Hence, the radial component of thermal radiation does not contribute to the error budget for the measurement of a putative near-constant, that is, very low-frequency, acceleration. By the placement of the radiators so that the heat they dissipate does not

produce a net force along the spacecraft axis, the contribution of the radiation force of heat can be reduced to a few watts. Note that the avoidance of reflections is much superior to the precision modeling of the thermal radiation characteristics of the spacecraft because the effect of surface deterioration during the journey is difficult to model. Thus, the avoidance of reflections by restricting the opening angle of radiators is mandatory for a precision test of the Pioneer anomaly. The radiation from other surfaces of the spacecraft can be monitored to some extent by measurements of the surface temperature. This option is discussed later for the case of the RTGs. Therefore, we will assume as a spacecraft design requirement that radiators are positioned in such a way as to reduce the total force due to the radiated heat along the spacecraft spin axis to a fraction of the Pioneer anomaly. We will set $\Delta a_{\text{bus}} = 1 \times 10^{-11}$ m/s^2.

By far the bigger source of thermal radiation are the RTGs, necessary to power the spacecraft systems. In particular, if one chooses an electrical-propulsion system, the thermal heat to be dissipated from the RTGs may easily reach 10 kW for the exploration paradigm.[52] In principle, an anomaly caused by RTG heat can be distinguished from other sources because it will exponentially decay with the 87.7 years of half-life of the plutonium, which would result in a change of approximately 8% in 10 years. In the case of the Pioneer spacecraft however, the disturbances by attitude-control maneuvers were so large that no reliable determination of a possible slope of the anomaly could be performed.[6] For a new mission, in which gas leaks are well under control, a reliable measurement should, however, be possible. Nevertheless, it is desirable to have an independent upper limit on the effect of RTG heat so that a reliable estimate can be given of this effect for each interval between attitude-control maneuvers.

Hence, it is preferable to reduce forces due to nonisotropic heat emission from the RTG to the level of a fraction of the expected anomaly. To accomplish this, RTG heat must be dissipated fore–aft symmetrically and reflections from the spacecraft should be avoided. This may be simply achieved by putting the RTGs on long booms or reducing their view factor toward other components of the spacecraft by a more intricate design. In combination with a detailed model of the radiation characteristics, this reduces any unmodeled directional heat radiation resulting from asymmetry to affordable values.

More troublesome is the effect of possible material degradation on the radiation characteristics of the RTGs. During a typical mission, the antenna-facing side of the RTGs will be exposed to solar radiation almost permanently, whereas the other side of the RTGs lies in shadow for nearly all of the mission. Hence, one can expect a very asymmetric degradation of the emissivity and absorptance of the RTGs. Whereas it would be difficult to predict which part of the RTGs surface degrades faster, most likely it would be the sun-facing side, one can reconstruct the overall degradation of the emissivity ϵ of the RTG by monitoring its temperature T at selected points.

We demonstrate the reconstruction of acceleration originating from degradation of optical properties of the RTG for a simplified model of a cylindrical RTG, with the cylinder axis perpendicular to the spacecraft–sun direction. As a further simplification, we assume perfect thermal conductivity of the RTG so that all of its surface is at the same temperature. We first derive a relation between the temperature and the emissivity change and then a relationship between the resulting change in acceleration and the emissivity change. We then show how under reasonable assumptions temperature and acceleration can also be directly related.

The azimuth angle ψ of the cylinder is measured from the sun-pointing direction. When the Stefan–Boltzmann law is used, the relation between the total radiated power P_{tot}, the emissivity per angle $\epsilon(\psi) = \epsilon_0 + \Delta\epsilon(\psi)$, and the temperature of the RTG is given by

$$P_{\text{tot}} = \frac{\text{const}\, T^4}{2\pi\epsilon_0} \int_0^{2\pi} [\epsilon_0 + \Delta\epsilon(\psi)]\, \mathrm{d}\psi$$

Because the thermal power produced by the RTG is well known from the amount of plutonium in it, the temperature of the RTG is directly related to change of emissivity $\Delta\epsilon$. Indicating with T_0 the temperature of the RTG when $\Delta\epsilon(\psi) = 0$, we have

$$T = T_0 \left[\frac{2\pi\epsilon_0}{2\pi\epsilon_0 + \int_0^{2\pi} \Delta\epsilon(\psi)\, \mathrm{d}\psi} \right]^{\frac{1}{4}}$$

On the other hand, the power per angle is related to the total radiated power by

$$P(\psi) = P_{\text{tot}} \frac{\epsilon_0 + \Delta\epsilon(\psi)}{\int [\epsilon_0 + \Delta\epsilon(\psi)]\, \mathrm{d}\psi} \tag{1}$$

The effective asymmetric power radiated along the spin axis of the craft is given by

$$P_a = \int_0^{2\pi} P(\psi) \cos(\psi)\, \mathrm{d}\psi \tag{2}$$

Inserting Eq. (1) into Eq. (2) and expressing the acceleration a_ϵ induced by the change in emissivity, we obtain

$$a_\epsilon = \frac{P_{\text{tot}}}{M_{\text{S/C}}\, c} \frac{1}{\int [\epsilon_0 + \Delta\epsilon(\psi)]\, \mathrm{d}\psi} \int_0^{2\pi} \cos(\psi)[\epsilon_0 + \Delta\epsilon(\psi)]\, \mathrm{d}\psi \tag{3}$$

In general, there will be no unique relation between T and a_ϵ because the quantities depend on different integrated functions of the emissivity. Nevertheless, a relation can be established under some reasonable model assumptions. To illustrate this, we consider an RTG that has an original emissivity of $\epsilon_0 = 1$, and we model the emissivity change with the simple relation

$$\Delta\epsilon(\psi) = -\Delta\epsilon_{\max} \cos(\psi), \qquad \text{for} \quad |\psi| \le \pi/2$$

where $\Delta\epsilon_{\max} > 0$ is the absolute value of the change of reflectivity in the sun-pointing direction. In this case, the deceleration of the spacecraft is given by

$$\Delta a_\epsilon = -(P_{\text{tot}}/4M_{\text{S/C}}c)\Delta\epsilon_{\max}$$

The temperature after the degradation of emissivity is then related to the temperature at nominal emissivity T_0,

$$T = (T_0/4\pi)\Delta\epsilon_{\max} + \mathcal{O}\left(\Delta\epsilon_{\max}^2\right)$$

We obtain the final relation

$$a_\epsilon = -(\pi P_{\text{tot}}/cM_{\text{S/C}})(T/T_0) \tag{4}$$

Consequently, we find for the acceleration uncertainty Δa_ϵ a dependence on the temperature uncertainty ΔT,

$$\Delta a_\epsilon = (\pi P_{\text{tot}}/cM_{\text{S/C}})(\Delta T/T_0)$$

For an RTG, the nominal temperature is $T_0 \sim 500$ K. Hence, assuming that we monitor the RTG temperature at a precision of 0.1 K and assuming the preceding degradation model, we would have an uncertainty in the anomalous acceleration of $\Delta a_\epsilon = 2.8 \times 10^{-11}$ m/s^2 for the exploration scenario and $\Delta a_\epsilon = 1.4 \times 10^{-11}$ m/s^2 for the piggyback scenario.

A realistic model of the RTG is considerably more complicated. It has to include the absorptance and to account for a nonuniform temperature of the RTG and the Yarkovsky effect (see Cruikshank[58] or Peterson[59]). These are, however, mainly numerical complications, and it is always possible to develop a refined version of Eq. (4) so that the uncertainty of the RTG temperature measurements may be related to the uncertainty of the derived acceleration. In particular, there is no danger of mistaking a degradation or failure of thermocouples of the RTG for a change in emissivity because these effects are distinguishable by the accompanying decrease of electric power. Hence, we assume that the acceleration levels found in the simple model are also achievable in a realistic situation.

D. Radio-Beam Radiation Force

The increasing amount of data gathered by modern planetary observation instruments demands high data transmission capabilities. For exploration missions to the outer solar system such as the ones discussed here, this inevitably leads to high transmission powers for the telecommunication system, $P_{\text{radio}} \sim 50$ W. Analogous to the case of thermal radiation, discussed in the preceding section, the acceleration on the spacecraft is given by

$$\boldsymbol{a}_{\text{radio}} \approx (P_{\text{radio}}/cM_{\text{S/C}})\boldsymbol{e}_A$$

in approximation of a narrow radio beam. Hence, it may easily reach the order of magnitude of the Pioneer anomaly. However, this bias can be constrained in a straightforward way. During the coast phase, in which the Pioneer anomaly is to be tested, the data volume generated onboard will be much smaller than at the final destination of the probe. Hence, the transmission power can be reduced to a few watts during the test, bringing the uncertainty in the transmission power for both mission paradigms down to less than 1 W. This would correspond to an acceleration systematic below $\Delta a_{\text{radio}} = 5 \times 10^{-12}$ m/s^2 for the planetary exploration mission and $\Delta a_{\text{Radio}} = 2.2 \times 10^{-11}$ m/s^2 for the microspacecraft. These numbers might be even further reduced by changing the transmission power to different values during the measurement period and measuring the subsequent change of the spacecraft acceleration. In this way, one could actually calibrate for the effect of the radiation beam.

E. Solar Radiation Pressure

The last major contribution to discuss in this context is the solar radiation pressure. For the present level of analysis, it is sufficient to discuss the effect of the solar radiation force by considering the force on a flat disk of the size of the spacecraft antennas and covered with white silicate paint. To further simplify our consideration, we restrict ourselves to specular reflection and neglect diffuse reflection and the Yarkovsky effect. Then we can express the acceleration induced by solar radiation pressure as[60]

$$\boldsymbol{a}_{\odot} = (P_{\odot}/cr^2)(A_{\text{S/C}}/M_{\text{S/C}})(1+\eta)\cos^2\theta \boldsymbol{e}_A \tag{5}$$

where we have used the fact that the tangential force arising from the partial specular reflection has no effect on the center-of-mass motion of the spacecraft due to the spin stabilization. Because the antenna is oriented toward Earth, the vector $\boldsymbol{e}_A$ is Earth pointing, and the two vectors $\boldsymbol{e}_A$ and $\boldsymbol{e}_{\odot}$ only enclose a small angle θ for large heliocentric distances, that is, in all mission options for most of the measurement phase (Sec. VI). The uncertainty of the acceleration due to solar radiation $\Delta\boldsymbol{a}_{\odot}$ is dominated by a possible change in the reflectivity properties of the spacecraft. We assume $\Delta\eta/\eta_0 = 5\%$. The uncertainties of all other quantities are about one order of magnitude smaller and can be neglected for our purposes. Hence, we find from Eq. (5) the acceleration uncertainty due to solar radiation pressure,

$$\Delta\boldsymbol{a}_{\odot} = (P_{\odot}/c\,r^2)(A_{S/C}/M_{S/C})\cos^2\theta \boldsymbol{e}_A \Delta\eta \tag{6}$$

The maximal value is taken for $\cos\theta = 1$. For the planetary exploration scenario, we find $\Delta a_{\odot} = 149(R_{\oplus}/r)^2 \times 10^{-11}$ m/s^2, and for the piggyback concept, $\Delta a_{\odot} = 268(R_{\oplus}/r)^2 \times 10^{-11}$ m/s^2. We see from these numbers that the uncertainty on the solar radiation force model would exceed one-third of the putative anomaly at heliocentric distances of less than 3 AU for the microspacecraft and 2 AU for the exploration mission. Below these heliocentric distances, a reliable detection of the anomaly would become impossible.

F. Summary of the Onboard Error Sources

In the preceding section, we discussed the major sources of systematic effects on the spacecraft acceleration for the two nondedicated concepts under consideration, and we have determined the uncertainties to which they can be restricted by suitable design measures. The numerical results are summarized in Table 2. For a spin-stabilized craft, all acceleration uncertainties arise along the rotational axis of the spacecraft, with the exception of the solar radiation pressure.

Table 2 Acceleration uncertainties for two mission paradigms

Head	POP paradigm Δa, (10^{-11} m/s^2)	Microspacecraft Δa, (10^{-11} m/s^2)
Fuel leaks	0.4	0.2
Heat from bus	1.0	1.0
Heat from RTG	2.8	1.4
RTG helium outgassing	2.7	2.0
Radio beam	0.5	2.2
Solar radiation pressure	$149\,(R_{\oplus}/r)^2\cos^2\theta$	$268\,(R_{\oplus}/r)^2\cos^2\theta$
Total	$7.4 + 149\,(R_{\oplus}/r)^2\cos^2\theta$	$6.8 + 268\,(R_{\oplus}/r)^2\cos^2\theta$

The sources of acceleration, which were identified, are uncorrelated, at least to the level of the modeling performed, and the overall acceleration due to systematics is, therefore, bounded by the value

$$\Delta a = \sum_i \Delta a_i$$

This returns $\Delta a = [7.4 + 149\,(R_{\oplus}/r)^2\cos^2\theta] \times 10^{-11}$ m/s^2 for the exploration mission and $\Delta a = [6.8 + 268\,(R_{\oplus}/r)^2\cos^2\theta] \times 10^{-11}$ m/s^2 for the piggyback microspacecraft. When sufficiently far from the sun, this would only, allow determination of the anomaly to a precision of 10%, which is approximately one order of magnitude worse than the error-budget presented by Nieto and Turyshev[7] for a highly symmetric dedicated spacecraft.

The accuracy to which an anomalous acceleration can be determined will also strongly depend on its direction. Because all error sources will cause an acceleration purely along the spin axis of the spacecraft, they will be competing with an Earth-pointing anomaly, which would most likely be an effect on the radio signal. When studying the capabilities of the mission to discriminate the direction of the anomaly, the systematic errors do not influence the result because their direction does not change and their magnitude has a gradient that cannot be confused with a direction-dependent modulation.

G. Summary of Spacecraft Design

From the goal to minimize the uncertainties in conventional accelerations, we have arrived at several design requirements for our spacecraft: Spin stabilization of the spacecraft seems mandatory to reduce the number of attitude-control maneuvers of the spacecraft. Furthermore, it ensures that all onboard-generated accelerations are pointing along the spin axis of the craft. This effectively eliminates the effect of systematics on the determination of the direction of a putative anomaly (Sec. V.D). For the exploration scenario, spin stabilization is most practically only chosen during the coast phases of the mission. An electric-propulsion system turns out to be the most promising option to reduce the amount of acceleration systematics from propellant leakage, although an electric-propulsion system has the disadvantage that, due to its high-power consumption, it considerably increases the amount of heat generated onboard the spacecraft. The major sources of asymmetric thermal radiation from the craft are the RTGs. The heat systematics can be constrained to a sufficient degree by monitoring the temperature of the RTGs. Furthermore, the view factor of the RTGs from the spacecraft bus and the antenna should be made as small as possible to reduce radiation backscattering and simplify the modeling. To constrain the systematics induced by the radio transmission beam, the transmission power during the measurement phase can be reduced to a few watts.

Whereas the requirements imposed on the spacecraft make it necessary that the spacecraft be designed with the goal of testing the Pioneer anomaly under consideration, the modifications suggested come at no increase in launch mass and at no increase in risk. In particular, the goal of testing the Pioneer anomaly is compatible with

Table 3 Sources of acceleration uncertainties and possible design solutions

Source of acceleration uncertainty	Suggested countermeasure
Thrust history uncertainty	Spin stabilization
Fuel leaks	Electric propulsion
Heat from spacecraft bus	Placement of radiators, spin stabilisation
Heat from RTGs	Reconstruction from monitoring of RTG temperature
RTG helium outgassing	Orientation of pressure relief valves on RTGs
Radio beam force	Low transmission power during test
Solar radiation pressure	Sufficient heliocentric distance

the constraints of a planetary exploration mission. The uncertainty sources and counter-measures are listed in Table 3.

V. Measurement Strategies

A. Instrumentation Options

A mission to test the Pioneer anomaly has to provide three types of information. It must monitor the behavior of the tracking signal for an anomalous blueshift it must be able to detect an anomalous gravitational force acting on the spacecraft, and it must also be capable of detecting an anomalous nongravitational force on the spacecraft. From these three tasks, it is obvious that radio tracking is the experimental method of choice because it is sensitive to all three of the possible sources of the Pioneer anomaly. Radio tracking will be analyzed extensively in the Secs. V.B–V.D.

However, the orbit reconstruction from radio-tracking data does not discriminate between a nongravitational systematics and a gravitational new physics origin of the anomaly. Such conclusions can only be drawn from a statistical test of a specific candidate model against the observed deviation from the nominal orbit. Hence, a model-independent discrimination between a gravitational and nongravitational anomaly would be highly desirable. Such a distinction could, in principle, be accomplished with an accelerometer onboard the spacecraft because deviations of the spacecraft from a geodesic motion will be induced by nongravitational forces only. Unfortunately, the use of accelerometers reaching the sensitivity level of the Pioneer anomaly is excluded by weight constraints: High-precision accelerometer assemblies weigh typically in the order of 100 kg, compare, for example, ESA's GOCE mission.[61] Thus the discrimination between a gravitational and nongravitational anomaly will rely on the interpretation of the tracking data.

To improve our understanding of disturbing forces generated by the space environment in the outer solar system, and to make sure that they cannot contribute significantly to the Pioneer anomaly, it is desirable to include a diagnostics package in the payload, consisting of a neutral and charged atom detector and a dust analyzer. The mass of such a package is approximately 1.5 kg (Ref. 56). Most likely it would be part of the payload due to space science interests anyway, as in the case of the New Horizons mission.[46]

B. Tracking Methods

We briefly review the available tracking methods to explain how their combination allows an unambiguous discrimination between the various possible causes of the anomaly. (See Thornton and Border[62] for an introduction to tracking methods.)

In sequential ranging, a series of square waves is phase modulated onto the uplink carrier. The spacecraft transponds this code. The ground station compares the transmitted and the received part of the signal and determines the round-trip time from the comparison. Because the modulated signal is recorded and compared to obtain the distance from the spacecraft to the ground station, the information obtained relies on the group velocity of the signal. The group velocity is influenced by the interplanetary plasma, which acts as dispersive medium, but not by gravitational effects, which are nondispersive. For this technique, we assume a range error $s_{\text{track}} = 0.6$ m at 1σ confidence level in our analysis.[62]

Doppler tracking uses a monochromatic sinusoidal signal. The signal is sent to the spacecraft and is coherently transponded back to Earth. The phases of both the outgoing signal and the incoming signal are recorded. Because the frequency of the wave is the derivative of the phase, the frequency change between the outgoing and incoming wave can be determined, and the relative velocity of the spacecraft and the tracking station can be inferred. The position is then obtained by integrating the observed velocity changes to find the distance between the spacecraft and the tracking station. The Doppler data are sensitive to other phase-shifting effects such as the frequency shift by the interplanetary plasma and to a gravitational frequency shift. For a long integration time, the Doppler error is usually dominated by plasma noise, which typically leads to an error of approximately $v_{\text{track}} = 0.03$ mm/s at 1σ confidence level.[62,63]

The simultaneous use of both tracking techniques allows for a correction of charged medium effects because for a signal that propagates through a charged medium the phase velocity is increased, whereas the group velocity is decreased by the same amount.[64] The comparison of the Doppler and ranging measurements to determine plasma effects has important benefits for nondedicated test of the Pioneer anomaly because it allows a determination of the errors induced by the charged interplanetary medium without requiring dual-frequency capabilities and is, thus, a considerable mass saver. Because the information of the sequential ranging relies on the group velocity of the signal, and the information of the Doppler tracking relies on the phase velocity of the carrier, the use of both ranging methods also allows distinction between a real acceleration of the spacecraft and an anomalous blueshift. Whereas a real acceleration would show up in both data, the frequency shift would only affect the Doppler signal, which is sensitive to changes in the phase velocity of the wave but not to the sequential ranging signal that measures the group velocity.

Both Doppler tracking and sequential ranging are primarily sensitive to the projection of the spacecraft orbit onto the Earth–spacecraft direction. To characterize a putative anomaly, it is, however, crucial to determine its direction. In view of this problem, it could be beneficial to obtain independent information on the motion of the spacecraft orthogonal to the line of sight. This information is in principle provided by delta differential one-way ranging (ΔDOR). Differential one-way ranging determines the angular position of a spacecraft in the sky by measuring the runtime difference of a signal from the spacecraft to two tracking stations on Earth. When it is assumed that the rays from the spacecraft to the two stations are parallel to each other, the angle between the spacecraft direction and the baseline connecting the two stations can be determined from the runtime difference. In ΔDOR, the accuracy of this method is further improved by differencing the observation of the spacecraft from that of an astronomical radio source at a nearby position in the sky. The typical accuracy achievable with ΔDOR is $\alpha_{\text{track}} = 50$ nrad at 1σ confidence level.[62] An improvement in accuracy of two orders of magnitude in angular resolution would be achievable if the next-generation radio-astronomical interferometer, the Square Kilometre Array, could be used for the tracking.[65] However, this observatory is not likely to be completed by the launch dates under consideration. Hence, we do not include this enhanced capability in our analysis.

C. Tracking Observables for the Pioneer Anomaly Test

The suitability of an interplanetary trajectory for a test of the Pioneer anomaly may be influenced by a dependence of the Pioneer anomaly on the orbital parameters of the trajectory, as already discussed in Sec. II.D. The second important criterion for the choice of trajectory is if it enables a precise measurement of the properties of the anomaly. For the purpose of a general survey of trajectory options for a broad class of missions, a simulation of the tracking performance for each trajectory becomes unfeasible due to the large computational effort involved. Hence, we resort to the opposite route: In this section we derive a linearized tracking model for the anomaly that neglects the backreaction of the anomaly on the orbital parameters of the trajectory. This model allows to express the performance of the tracking techniques for a specific trajectory as a function of the heliocentric distance of the spacecraft and the flight angle only.

The capabilities of the three tracking techniques are evaluated by determining after which time a detectable deviation from the trajectory has accumulated. The perturbation on the position vector is well described, for our purposes, by the simple equation

$$\ddot{\boldsymbol{s}}^* = \boldsymbol{a}^* \tag{7}$$

where $\boldsymbol{s}^* = \boldsymbol{r} - \boldsymbol{\rho}$ is the difference between the position $\boldsymbol{r}$ of a spacecraft not affected by the anomaly and the position $\boldsymbol{\rho}$ of a spacecraft affected by the anomalous acceleration $\boldsymbol{a}^*$. In fact, we may write (Bate et al.[66]) the full equation of motion in the form

$$\ddot{\boldsymbol{s}}^* + (\mu_\odot/r^3)[(r/\rho)^3 - 1]\boldsymbol{r} + \mu_\odot(\boldsymbol{s}^*/\rho^3) = \boldsymbol{a}^* \tag{8}$$

Note that this holds also for non-Keplerian $\boldsymbol{r}$ whenever the nongravitational modeled forces may be considered state independent (as is the case for the systematic accelerations considered in Sec. IV.F). At Jupiter distance, it takes roughly three months for the second and third terms of Eq. (8) to grow within two orders of magnitude of $\boldsymbol{a}^*$. The smallsize of the backreaction on the orbital parameters is also the reason why it is not possible to decide from the Pioneer Doppler data if the observed anomaly is caused by an effect on the radio signal or a real acceleration. Thus, Eq. (7) and its solutions,

$$\boldsymbol{v}^* = \int_{t_0}^{t_1} \boldsymbol{a}^*(t')\,\mathrm{d}t', \qquad \boldsymbol{s}^* = \int_{t_0}^{t_1}\int \boldsymbol{a}^*(t')\,\mathrm{d}t' \tag{9}$$

can be used to estimate the deviation from the nominal trajectory caused by the anomaly.

Without loss of generality, we consider our spacecraft as lying in the ecliptic plane. The geometry for this two-dimensional model is shown in Fig. 1. Direct connection to the tracking observations in the geocentric frame, in which the measurements are actually conducted, can be established by projecting the anomalous velocity change and position change onto the Earth–spacecraft vector. (For our purposes, we can neglect the purely technical complications arising from the geocentric motion of the tracking stations. See, for example, Montenbruck and Gill,[17] for an extensive discussion of this topic.) The change in the geocentric angular position of the spacecraft in the sky, $\alpha^*_\oplus$, is obtained from the component of $\boldsymbol{s}^*$ perpendicular to the Earth–spacecraft direction through the relation $\alpha^*_\oplus \simeq s^*_\perp/s$. We obtain

$$v^*_\parallel = |v^*(t_1)|\cos\beta(t_1) - |v^*(t_0)|\cos\beta(t_0) \tag{10}$$

$$s^*_\parallel = |s^*(t_1)|\cos\beta(t_1) - |s^*(t_0)|\cos\beta(t_0) \tag{11}$$

$$\alpha^*_\oplus \simeq [1/s(t_0)][|s^*(t_1)|\sin\beta(t_1) - |s^*(t_0)|\sin\beta(t_0)] \tag{12}$$

where β is the angle between the anomaly direction and the Earth–spacecraft vector. Equations (10–12) estimate the effect an anomalous acceleration on the tracking observables. Note that the magnitude of the Doppler observable only grows linearly with time, whereas the observables of ranging and ΔDOR grow quadratically in time.

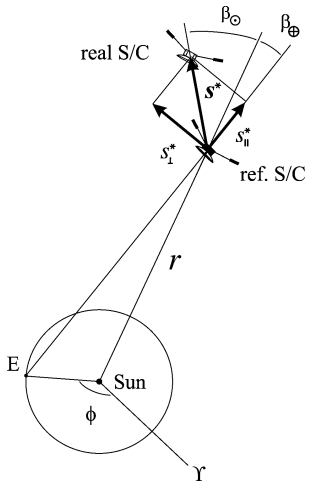

Fig. 1 Tracking of anomaly in ecliptic plane.

It is convenient to express the angle β as the sum of the angle between $\boldsymbol{a}^*$ and the sun–spacecraft vector $\beta_\odot$ and the angle between the Earth–spacecraft vector and the sun–spacecraft vector $\beta_\oplus$ (Fig. 1),

$$\beta = \beta_\odot + \beta_\oplus$$

With this decomposition, several relevant cases can easily be treated: First is the case of sun-pointing acceleration from a central force, $\beta_\odot \equiv 0$. Second is the case of inertially fixed acceleration $\beta_\odot = \text{const}$. This case also yields insights into the case of a drag-force-type deceleration along the trajectory because the change of $\beta_\odot(t)$ typically stays within the same magnitude as that of $\beta_\oplus(t)$. Third is the case of a blueshift of light. It leads only to a change of the apparent velocity along the line of sight of the spacecraft, $v^*_\parallel$, but not of the position $\boldsymbol{s}^* \equiv 0$. From the direction of the effect, we have immediately $\beta \equiv 0$.

Both the rate of change $\dot{\beta}_\odot$ and the angle $\beta_\oplus$ are small quantities for trajectories in the outer solar system. Hence, analytical expressions for $\cos\beta$ and $\sin\beta$ are conveniently obtained by expanding β around the angle at the beginning of the tracking interval $\beta(t_0)$ in the quantities $\dot{\beta}_\odot$ and the mean motion of the Earth. After these steps, the magnitude of the anomalous components of the tracking observables in the preceding cases of special interest depends on the heliocentric distance r and the direction of the anomaly in the heliocentric frame $\beta_\odot$ only.

Expressions analogous to Eqs. (10–12) and the expansions described earlier hold for the systematic acceleration uncertainties summarized in Sec. IV.F. Combining the expressions for the effect of the anomaly and the systematic accelerations, one can determine the sensitivity of a tracking technique to one of the three generic classes of the Pioneer anomaly.

D. Tracking Performance

We content ourselves with the evaluation of the tracking performance for an anomaly of constant magnitude as indicated by the Pioneer data. The measurement performance is conveniently evaluated by splitting the change in the generic tracking observable f induced by the anomaly into a constant component f^* and a time-dependent component δf^* that is dependent on the direction in which the anomaly acts.

First we consider the detectability of the anomaly without attempting to determine its direction. For this goal, it is sufficient to consider the zeroth-order terms in the expansion around $\beta(t_0)$. For the anomaly to be detectable, term f^* has to exceed the measurement error. The measurement error, in turn, is given by the sum of the tracking error (where we require a confidence level of 3σ) and the uncertainty in the systematic accelerations Δf. The two errors have to be added instead of taking their Pythagorean sum because the error induced by the uncertainty in the systematic accelerations is not of statistic nature. Thus, the condition for detectability reads

$$f^* > f_{\text{track}} + \Delta f \tag{13}$$

We first consider the case of Doppler tracking, $v^*_\parallel > v_{\text{track}} + \Delta v$. Solving for the tracking time, we find

$$t_v > v_{\text{track}}/(a^*\cos\beta_\odot - \Delta a)$$

Proceeding analogously for sequential ranging and ΔDOR, one finds that sequential ranging and Doppler tracking easily detect an anomaly of $a^*\cos\beta_\odot = 10^{-9}$ m/s^2 within two days of tracking at heliocentric distances beyond Jupiter's orbit. The time to detection decreases slightly for larger heliocentric distance due to the decrease of the solar radiation pressure. ΔDOR cannot compete in performance with the other tracking methods. Even if we consider $a^* = 10^{-9}$ m/s^2 and $\beta_\odot$ as large as 30 deg, the detection of the anomaly takes 140 days even at 5 AU and rises to 370 days at 35 AU.

Significantly more challenging than the detection of the anomaly is the determination of its direction. Here, we consider the detection

of the three most plausible candidate directions: sun pointing, along the velocity vector, and Earth pointing. The case of an acceleration along the velocity vector is, to a good approximation, covered by the case of an acceleration having a fixed angle with the sun–spacecraft vector because the change of the flight angle of the spacecraft along the trajectory will be very slow.

A sun-pointing effect would be revealed by the variation of the tracking observables due to the Earth's rotation around the sun. To detect unambiguously the annual modulation δf in a tracking observable f, its modulation has to exceed the sum of the tracking error f_{track} and of the uncertainty in the annual modulation of systematic accelerations $\delta(\Delta f)$,

$$|\delta f_{\parallel}^{*}| > f_{\text{track}} + |\delta(\Delta f_{\odot})| \tag{14}$$

The systematics term stems entirely from the uncertainty in the solar radiation force, $\delta(\Delta f) = \delta(\Delta f_{\odot,\parallel})$, because all other accelerations are Earth pointing and do not show a modulation (cf. Sec. IV.F).

We set an upper limit of six months on the detection time because this is the expected approximate time span between two attitude-control maneuvers. Longer time spans cannot be evaluated in the search for the modulation because the attitude maneuvers are expected to considerably degrade our knowledge of the orbital motion of the spacecraft. Putting this limit on the observation time and using the error budget determined in Sec. IV.F, we find that the annual modulation is detectable by Doppler tracking up to 6.2-AU heliocentric distance for both the exploration spacecraft and for the microspacecraft. Applying the same reasoning for sequential ranging, one finds that for both paradigms the annual modulation remains detectable in sequential ranging beyond 50 AU. For ΔDOR, the modulation term is suppressed compared with the constant term, by a factor of $r_{\oplus}/r$. When the poor performance of ΔDOR for the constant term is considered, it is obvious that this method will not be capable of a standalone detection of any type of annual modulation.

Next we consider an anomaly that has a fixed angle $\beta_{\odot}$ with the sun–spacecraft direction. Again the only time-variable source of acceleration systematics is the uncertainty in the solar radiation force. We assume $\beta_{\odot} = 15$ deg, which relates to the value that we will consider as the maximal flight angle for the trajectories in the following section as $\gamma < 90$ deg $-\beta$. Limiting the tracking time to one year again, we find that Doppler tracking can detect this type of anomaly up to 23 AU for the exploration paradigm and up to 22 AU for the piggyback microspacecraft. Again sequential ranging is capable of detecting the modulation term beyond 50 AU for both paradigms, which is more than sufficient for the mission types under consideration.

In summary, sequential ranging proves to be the most powerful tracking technique for a verification of the Pioneer anomaly. In particular, the discrimination between the candidate directions of a putative anomaly can be performed by sequential ranging during the whole length of the interplanetary trajectories under consideration.

At first sight, this result seems in contrast with the common wisdom that range data are usually inferior in quality to Doppler data.[67] However, the standard situation, in which precision navigation is most relevant, is that of a planetary approach. In this case, the gravitational field is rapidly changing along the spacecraft orbit, and ranging data induce larger navigational errors than Doppler indeed. For the deep-space situation of the Pioneer anomaly test, the gravity gradients are very low, and hence, the reliability of sequential ranging data is much improved.

Doppler data will, nevertheless, be of high importance for the measurement. Only by the comparison of both data types, sequential ranging and Doppler, can one discriminate between a real acceleration and a blue shift of the radio signal.

ΔDOR showed to be of little use for a test of the Pioneer anomaly. In particular, it cannot resolve the directionality of the anomaly. Hence, although it is certainly desirable to have occasional ΔDOR coverage during the Pioneer anomaly test to verify the orbit reconstruction of the spacecraft (cf. Thornton and Border[62]), ΔDOR does not play a key role in the precision determination of the anomaly.

From the analysis of the various tracking techniques, we can also infer requirements on the trajectory of the spacecraft. A upper limit on the flight angle is desirable if the anomaly direction is supposed to be determined. In particular, the lowest-order modulation term signaling a velocity-pointing anomaly is proportional to the cosine of the flight angle. For flight angles close to $\gamma = 90$ deg, the ability to distinguish an anomaly along the velocity vector from other candidate effects is suppressed $\sim r_{\oplus}/r$. Hence, a reduced flight angle considerably improves the sensitivity to such an effect.

To now we have not touched on an effect that could crucially degrade our measurement accuracy. The preceding estimates assume that the spacecraft remains undisturbed during the measurement period necessary to detect the anomaly or its modulation. However, this presupposes that no engine firings are necessary within the time span of detecting the anomaly and, furthermore, that meteoroid impacts are rare enough to leave us with sufficient undisturbed measurement intervals to detect the modulation signals. Concerning thruster firings, this condition is in fact fulfilled. The major disturbance torque in deep space will be the solar radiation pressure. Even with a low rotation speed of 0.01 rpm, which we found beneficial for the exploration missions, the time span between thruster firings necessary to compensate for this disturbance will be in the order of months, leaving enough time to conduct precision measurements of the Pioneer anomaly. For the Pioneer 10 and 11 missions, no disturbances due to the gravitational fields of asteroids could be noticed. Hence, we can exclude this as a possible source of disturbance for our measurement. Analysis of the Pioneer tracking data also demonstrated that noticeable meteoroid impacts occurred only at a frequency of a few per year. We are not trying to account for a continuous stream of impacts of small dust particles that are not visible as single events in the tracking data. Rather, we consider such a stream as a putative source of the anomaly, which should in turn be recognized from its directionality.

VI. Trajectory Design

We have already discussed how the introduction of a momentum dependence of the gravitational coupling could explain why the Pioneer anomaly does not show in the planets ephemerides. Even more straightforwardly, an amplification of the anomaly at high velocities could occur if matter on low-eccentricity orbits around the sun causes a drag force. (Note, however, that there does not seem to be enough dust available.[2,68]) As a consequence, it is desirable to conduct the Pioneer anomaly test along a trajectory having a high radial velocity, that is, a hyperbolic escape trajectory, rather than on a bound orbit. Otherwise, the choice of the inclination, the argument of perihelion, and the longitude of the ascending node do not affect the test.

From the data of the Pioneer probes, no precise determination of the direction of the anomalous force was possible. This mainly followed from the fact that Doppler tracking is able to determine the velocity of a spacecraft only in the geocentric direction. In particular, it was not possible to distinguish between the three major candidate directions of the anomaly: toward the sun, toward the Earth, and along the trajectory. The uncertainty in the onboard generated accelerations, therefore, makes it desirable to design the spacecraft trajectory trying to obtain a large flight angle to facilitate the distinction between the candidate directions from the analysis of the tracking data (cf. the preceding section): Unfortunately this requirement is in conflict with the wish to have high radial velocity of the spacecraft and fast transfer times. A large flight angle could be obtained by conducting the Pioneer anomaly measurement as far inward in the solar system as possible. Unfortunately, the last requirement conflicts with the goal of having the smallest possible systematics generated by solar radiation pressure. A tradeoff between these conflicting requirements has to be made on a case-by-case basis and is here discussed for a number of representative trajectories. Because the Cosmic Vision Programme of ESA refers to the decade 2015–2025, this time span will be used as a baseline launch date for the trajectories here considered. Missions to Pluto, Neptune, and Uranus are discussed separately from those to Jupiter and Saturn because the distances of the former planets allow for a Pioneer anomaly test to be conducted by the exploration spacecraft during its long trip. For the latter two targets, one has to resort

to using a special microspacecraft piggybacked to the exploration spacecraft (Sec. III.C).

A. Orbiter Missions to Pluto, Neptune and Uranus

In this section, we discuss the possibility of using putative exploration missions to Pluto, Neptune, and Uranus to perform the Pioneer anomaly test. We will first consider simple flyby missions to these outer planets. These kind of missions are not too likely to happen because the scientific return of a flyby is quite limited and has already been exploited in several past interplanetary missions. Therefore, we will go one step further and consider orbiter missions exploiting nuclear electric propulsion for a final orbital capture. The trajectory baseline is that of one sole unpowered gravity assist around Jupiter. Many trajectory options and missions are of course possible for exploring these far planets, for example, that described by Vasile et al.,[69] but a single Jupiter swingby is probably the most plausible baseline in terms of risk and mission time. The purpose is to show that a Pioneer anomaly test would, in general, be possible on these missions, on the vast majority of the possible trajectories. In the considered mission scenario, the Pioneer anomaly test would be performed during the ballistic coast phase after Jupiter. A good trajectory from the point of view of the Pioneer anomaly test has the following characteristics (Sec. II.D): 1) hyperbolic trajectory, 2) reduced flight angle γ (where we will allow at maximum 75 deg) during the test (allowing easy distinction between the velocity direction and the spacecraft–Earth direction), 3) long ballistic phase, and large sun–spacecraft–Earth angle during the test (allowing distinction between the Earth direction and the sun direction).

We briefly touch on the implications of these requirements. From standard astrodynamics we know that along a Keplerian trajectory we have the following relation for the flight angle:

$$\cos\gamma = \sqrt{p}\Big/\left(r\sqrt{2/r - 1/a}\right)$$

where p is the semilatus rectum and a the semimajor axis of the spacecraft orbit. It is, therefore, possible to evaluate the flight angle γ at any distance from the sun by knowing the Keplerian osculating elements along the trajectory after Jupiter. In particular, we note that highly energetic orbits, that is, fast transfers, lead to larger values of the angle γ. This leads to the preference for a slower transfer orbit. However, a low velocity also results in a longer trip and might cause to a smaller value of the anomaly. The requirement on the length of the ballistic arc (an issue for orbiter mission baselines) also tends to increase the transfer time. In fact, the onboard propulsion (assumed to be some form of low thrust) could start to brake the spacecraft much later in a slower trajectory. (The square of the hyperbolic velocity $C3$ at arrival on a Lambert arc gets smaller in these missions for longer transfer times.) To have a large sun–spacecraft–Earth angle during the test phase implies that the test has to start as soon as possible after the Jupiter swingby, not allowing for a long thrust phase immediately after the swingby as would be required by optimizing some highly constrained trajectory for low-thrust orbiter missions. To assess the impact of the requirements on the trajectory design, we conduct a multi-objective optimization of an Earth–Jupiter–planet flyby mission, assuming pure ballistic arcs and an unpowered swingby. We evaluate the solutions using the Paretian notion of optimality, that is, a solution is considered as optimal if no other solution is better with respect to at least one of the objectives. We optimize the $C3$ at Earth departure, as well as the mission duration. (As discussed, this parameter is directly related to the flight-path angle and to the ballistic arc length.) The Earth departure date t_e, the Jupiter swingby date t_j, and the planet arrival date t_p were the decision variables, the departure date being constrained to be within the Cosmic Vision launch window and the arrival date being forced to be before 2100.

The optimization was performed using a beta version of the (distributed global multi-objective optimizer), DiGMO[70] a tool being developed within ESA by the Advanced Concepts Team. The software is able to perform distributed multi-objective optimizations with a self-learning allocation strategy for the client tasks. Differential evolution[71] was used as a global optimization algorithm to build the Pareto sets. Constraints were placed on the Jupiter swingby altitude ($r_p > 600{,}000$ km). Planet ephemerides were JPL DE405.

The results, shown in Fig. 2, show two main optimal launch opportunities for the Earth–Jupiter–Pluto transfer: November 2015 and December 2016. The 2015 launches result in a slower trajectory (from 17 to 27 years) with lower $C3$ (of the order of 87 km^2/s^2), whereas the 2016 window results in a shorter mission (from 11 to 15 years) with slightly higher $C3$ (of the order of 92–100 km^2/s^2). From a Pioneer anomaly test point of view, the only trajectories that would not allow a good test are the very fast transfers because the β angle may become as large as 75 deg by 25 AU. On the other trajectories, the test would be feasible and it would only affect the low-thrusting strategy because the test requires a long ballistic arc with no thrust phase immediately after Jupiter. This requirement is discussed later.

Similar results are obtained for the Neptune case (Fig. 3.) There are two optimal launch windows in the considered decade: January 2018 and February 2019. The first window allows for very low $C3$ (of the order of 75 km^2/s^2) and transfer times ranging from 14 to 40 or more years, whereas the second launch window is characterized

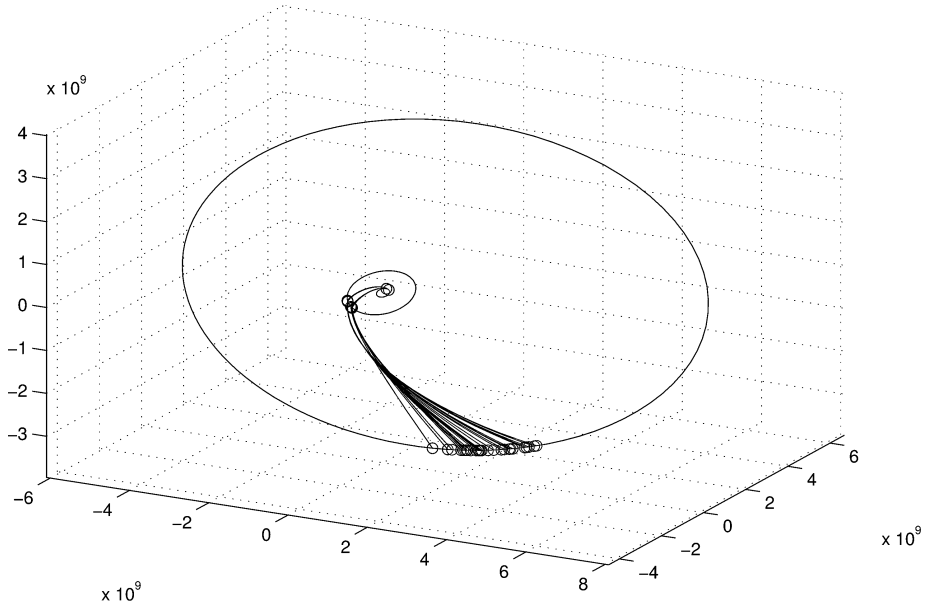

Fig. 2 Paretian set for Earth–Jupiter–Pluto mission within decade 2015–2025.

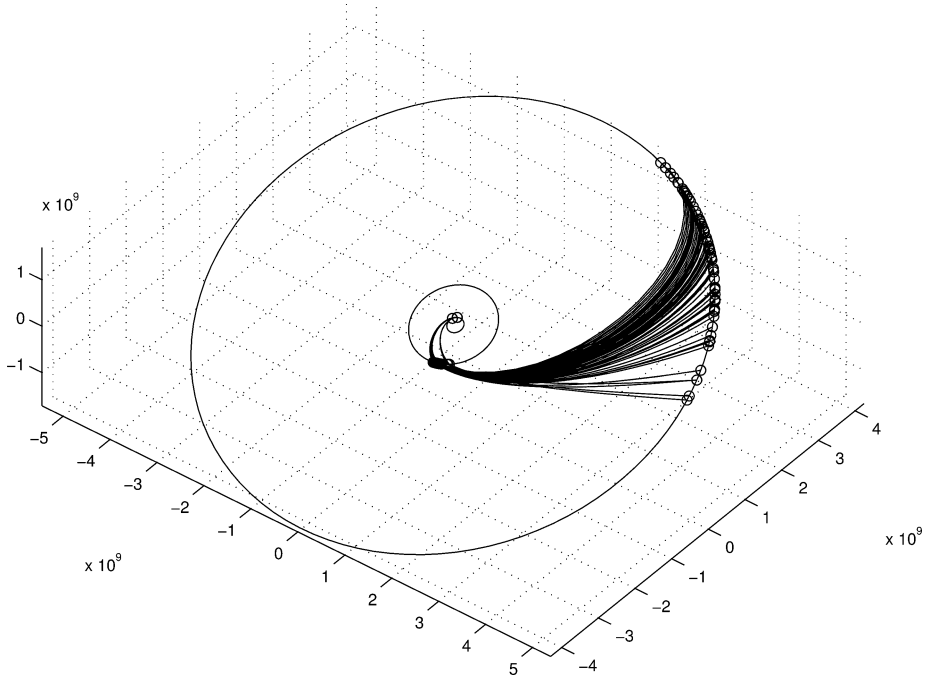

Fig. 3 Paretian set for an Earth-Jupiter-Neptune mission within the decade 2015–2025.

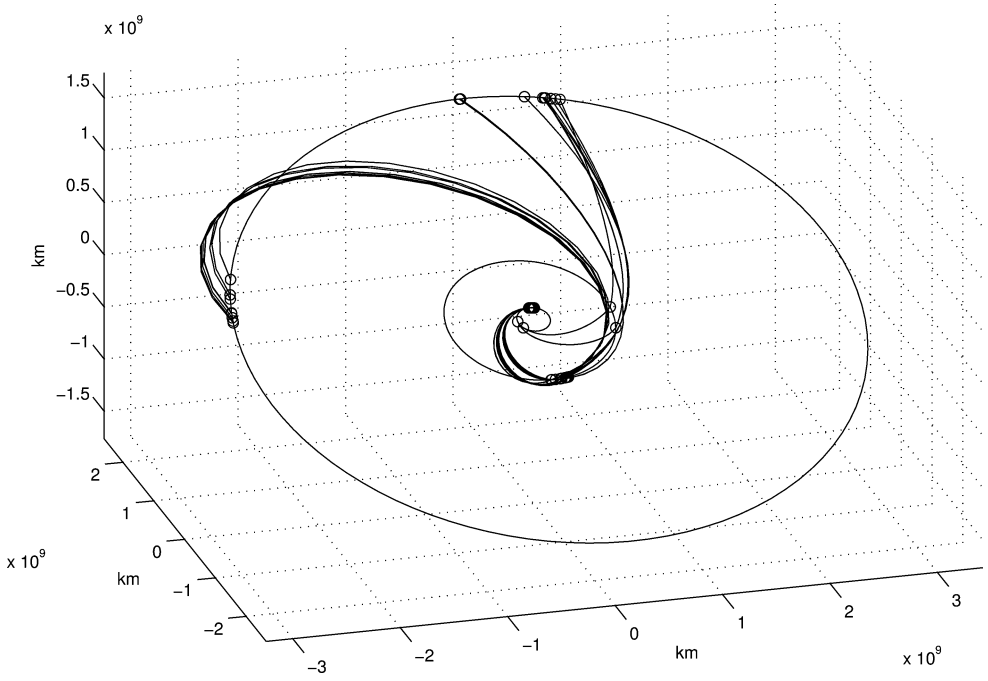

Fig. 4 Paretian set for Earth–Jupiter–Uranus mission within decade 2015–2025.

by higher $C3$ values (ranging from 90 to 95 km^2/s^2) and shorter mission times (as low as 10 years). The requirement on the β angle is, in this case, satisfied by all of the trajectories of the Pareto front.

The situation for Uranus missions, shown in Fig. 4, is slightly more complex. Three main launch windows are possible. The first one, corresponding to a late Jupiter flyby, is in March 2020 (repeating in April 2021) and corresponds to a $C3$ of roughly 81 km^2/s^2 (rising to 96 km^2/s^2 one year later) and to missions as short as 9 years. The other two are in December 2015 and December 2016, producing optimal first-guess trajectories with $C3$ of the order of 78–79 km^2/s^2 and transfer times that are either very high (33 years) or of the order of slightly more than a decade. Because of the vicinity of the planet in this case, the value of the flight angle is not an issue. Note that a hypothetical mission to Uranus exploiting one Jupiter flyby would probably use the 2020 launch opportunity, paying an augmented $C3$ cost of approximately 2 km^2/s^2 to reduce the mission time by several years. The conclusions of the preliminary multi-objective optimization are summarized in Table 4.

Each of the trajectories belonging to the Pareto fronts might be modified to allow an orbiter mission. Notwithstanding some concepts to navigate into deep space with solar electric propulsion, it seems that the nuclear electric option is the most convenient and has to be used if we want to navigate in the outer regions of the solar system. Starting from one of the trajectories of the Pareto front, if the launcher is able to provide all of the $C3$ that are required and we do not apply heavy constraints, the optimal trajectory will be ballistic up to the very last phase and a braking maneuver would start just before the arrival to the planet. If the problem is more constrained, for example, if we add a departure $C3$ upper limit, then the ion engines also would need to be fired before and after Jupiter. The firing

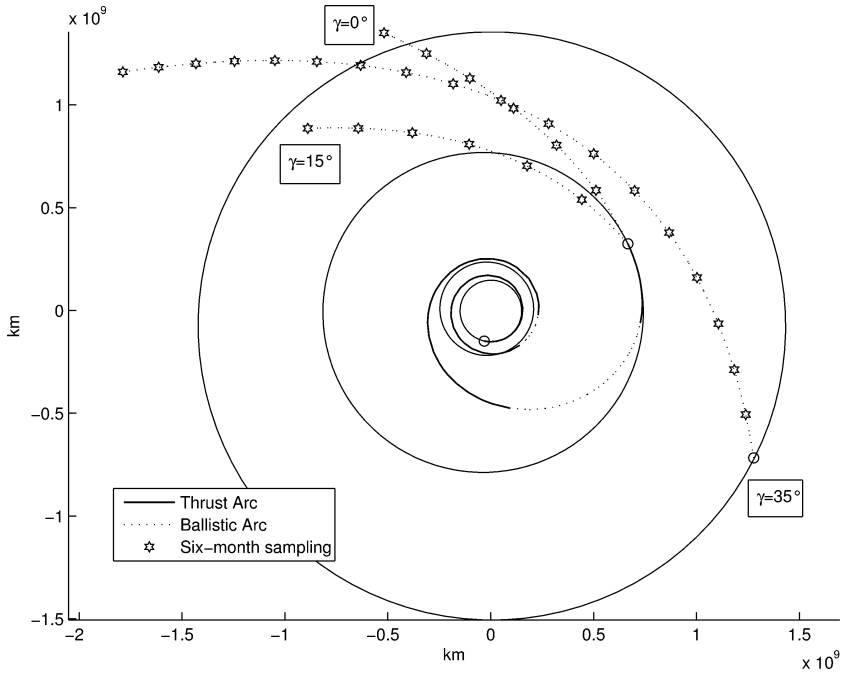

Fig. 5 Piggyback microspacecraft trajectory options.

Table 4 Pareto-optimal launch windows for flyby missions to various outer planets in considered decade

Target planet	Departure date	Mission duration, years	Departure $C3$, km^2/s^2
Pluto	Nov. 2015	17–27	89–88
Pluto	Dec. 2016	11–15	92–100
Neptune	Jan. 2018	14–40	74–75
Neptune	Feb. 2019	10–12	90–95
Uranus	March 2020	9	81
Uranus	April 2021	7	96
Uranus	Dec. 2015–2016	12–14	79
Uranus	Dec. 2015–2016	28–33	79

immediately after Jupiter is necessary to assure that Pluto orbit is reached at the right time. (This was the case for the POP trajectory to Pluto.[52]) In this case, a Pioneer anomaly test would return less scientific data because the thrusting phases could not be used for the characterization of the putative anomaly. Adding a constraint not to use the engines immediately after Jupiter, on the other hand, would introduce an increase in the propellant mass needed due to the late trajectory correction. This occurrence would hardly be accepted by the system designers, and anyway the Pioneer anomaly test would be possible during the subsequent coast phase of several years.

We may conclude that any trajectory of a flyby or of an orbiter mission to the outer planets Pluto, Neptune, and Uranus is likely to be suitable for a Pioneer anomaly test with no modifications, meaning that the three main requirements discussed would be fulfilled during a trajectory arc long enough to gain significant insight into the anomaly.

B. Microspacecraft Jettisoned from Jupiter and Saturn Missions

A different situation occurs if we try to test the Pioneer anomaly by exploiting a putative mission to Jupiter or Saturn. In these cases, the proximity of the planets to the sun and the likely low energy of the transfer orbit would not allow for the test to be performed during the travel to the planet. A possible solution is that of designing a piggyback microspacecraft to be added as a payload to the main mission. We already presented a preliminary assessment of the dry mass of such a payload in Sec. III.C, and we now discuss what the fuel requirement would be on such a spacecraft. As a guideline for the mother-spacecraft trajectory, we consider the JIMO baseline and perform an optimization of a 2016 launch opportunity. This was done to obtain information on the switching structure of the thrust so that possible strategies of jettisoning could be envisaged. The thrust is considered to be fixed and equal to 2 N for a spacecraft weighing 18,000 kg. Final conditions at Jupiter do not take into account its sphere of influence. The optimized trajectory (Fig. 5) foresees a June 2016 injection into a zero $C3$ heliocentric trajectory and a rendezvous with Jupiter in May 2023. We require that the microspacecraft secondary mission does not affect the mothercraft trajectory, optimized for the main mission goals. A feasible solution is a spacecraft detaching from the mother spacecraft at the border of the arrival-planet's sphere of influence, navigating toward a powered swingby of the target planet, and putting itself autonomously into a hyperbola of as high as possible energy. Some general estimates may then be made. We assume that the piggyback spacecraft is at the border of Jupiter's sphere of influence with zero $C3$. The gravity assist has to allow it to gain enough energy to have, in the heliocentric frame, a hyperbolic trajectory. We also allow for a nonzero flight angle γ at Jupiter. Under the assumption of a tangential burn at the periapsis (Gobetz[72]), we find for the required ΔV the expression

$$\Delta V = \sqrt{V_P^2(3 - 2\sqrt{2}\cos\gamma) + 2(\mu_P/r_{pP})} - \sqrt{2(\mu_P/r_{pP})} \quad (15)$$

Once the required ΔV is obtained from Eq. (15), it is easy to work out the ratio between the propellant mass and the spacecraft dry mass using the Tsiolkovsky equation. Assuming the use of chemical propulsion for the powered gravity assist ($I_{sp} = 260$ s) and putting a constraint on the gravity assist altitude of 600,000 km in the Jupiter case and 40,000 km in the Saturn case, one finds the ΔV and fuel-to-dry-mass ratio in dependence of the flight angle as shown in Table 5. Because of the high pericenter required and because of the greater velocity of the planet, the Jupiter case requires a higher propellant mass.

As a consequence, the same spacecraft designed for a $|\gamma| = 15$ deg Jupiter case is capable, in the Saturn scenario, to go into a $|\gamma| = 35$ deg trajectory. Figure 5 shows example hyperbolic trajectories that first go to decreasing heliocentric distances and have good performances with respect to the Pioneer anomaly test. They allow for long periods in which the direction of the anomaly could be precisely measured because the modulations in the tracking signal due to the motion of the Earth, which enable the determination of the direction of the anomaly, are enhanced for low heliocentric distances.

Table 5 Microspacecraft thrust requirements

	γ, deg								
XXXX	0	7.5	15	22.5	30	37.5	45	52.5	60
				Jupiter case					
ΔV, km/s	0.7	0.8	1.1	1.6	2.2	3	3.8	4.8	5.8
$\Delta M/M_0$	0.32	0.37	0.53	0.84	1.3	2.2	3.5	5.6	8.9
				Saturn case					
ΔV, km/s	0.17	0.2	0.27	0.39	0.55	0.76	1	1.3	1.6
$\Delta M/M_0$	0.071	0.081	0.11	0.17	0.24	0.35	0.48	0.65	0.86

VII. Conclusions

We have considered two plausible mission architectures for the exploration of the outer solar system that may also be used to test the Pioneer anomaly. First, a class of low-mass low-thrust missions to Pluto, Neptune, or Uranus. For this mission type, the Pioneer anomaly investigation can be performed by radio tracking of the exploration spacecraft. The other mission paradigm considered is that of a microspacecraft piggybacked on a large nuclear-reactor-powered spacecraft sent to explore Jupiter or Saturn. The small spacecraft would be jettisoned from the mothercraft on the approach to its destination, would use the target planet of the mothercraft for a powered swingby, and subsequently performs the Pioneer anomaly investigation by radio tracking on a hyperbolic coast arc. Starting from a review of our knowledge of the effect and the models for its explanation, we have derived a set of minimal requirements for the spacecraft design and trajectory.

For both mission paradigms, the detection of the anomaly is found to be possible during the whole measurement phase, which extends over several years. Onboard systematics would still limit the precision in the determination of the magnitude of the anomaly to approximately 10%. This does not seem much of an improvement compared to the 15% error margin of the original determination from Pioneer 10 and 11 tracking data. However, by using suitable system design solutions, a nondedicated test would be able to rule out the last candidate onboard sources of the anomaly. Furthermore, the simple requirement of a minimal flight angle for the trajectories enables the discrimination between the most plausible classes of candidate models for the anomaly. The attainable acceleration sensitivity of $\sim 8 \times 10^{-11}$ m/s^2 will be insufficient for a precise characterization of the anomaly. In particular, a slope of the anomaly would most likely only be determined to the first order, if at all. This would hardly be sufficient to determine unambiguously the physical law that might underlie the Pioneer anomaly. Hence, the quality of the scientific return of nondedicated missions cannot compete with a dedicated mission for which acceleration sensitivities down to 10^{-12} m/s^2 would be attainable. In view of the ongoing controversial discussion about the origin of the Pioneer anomaly and the extraordinary costs of a dedicated deep-space mission to the outer solar system, however, it seems more appropriate to consider the more modest approach of using a nondedicated mission to verify if the Pioneer anomaly is indeed an indication of a novel physical effect.

Acknowledgments

The authors are grateful to Charles Walker at NASA Launch Services for providing them the Jet Propulsion Laboratory ephemerides MATLAB® routines. This work has much benefitted from discussions with Denis Defrère, Tiziana Pipoli, Roger Walker, Diego Olmos Escorial, Michael Martin Nieto, and Slava G. Turyshev.

References

[1]Anderson, J. D., Laing, P. A., Lau, E. L., Liu, A. S., Nieto, M. M., and Turyshev, S. G., "Indication, from Pioneer 10/11, Galileo, and Ulysses Data, of an Apparent Anomalous, Weak, Long-Range Accelerattion," *Physical Review Letters*, Vol. 81, 1998, pp. 2858–2861; also http://arxiv.org/abs/gr-qc/9808081.

[2]Anderson, J. D., Laing, P. A., Lau, E. L., Liu, A. S., Nieto, M. M., and Turyshev, S. G., "Study of the Anomalous Acceleration of Pioneer 10 and 11," *Physical Review*, Vol. D65, 2002, pp. 082004-1–082004-50; also http://arxiv.org/abs/gr-qc/0104064.

[3]ESA Fundamental Physics Advisory Group, "Recommendation on the 'Cosmic Vision' Programme," Technical Rept. FPAG(2004)10, ESA, 2004.

[4]Lasher, L., and Dyer, J., "Pioneer Missions," *Encyclopedia of Astronomy and Astrophysics*, edited by P. Murdin, Inst. of Physics, Bristol, England, U.K., 2002; also http://eaa.iop.org/abstract/0333750888/2187.

[5]Null, G. W., "Gravity Field of Jupiter and Its Satellites from Pioneer 10 and Pioneer 11 Tracking Data," *Astronomical Journal*, Vol. 81, 1976, pp. 1153–1161.

[6]Markwardt, C. B., "Independent Confirmation of the Pioneer 10 Anomalous Acceleration," 2002, http://arxiv.org/abs/gr-qc/0208046.

[7]Nieto, M. M., and Turyshev, S. G., "Finding the Origin of the Pioneer Anomaly," *Classical and Quantum Gravity*, Vol. 21, 2004, pp. 4005–4024.

[8]Katz, J. I., "Comment on Indication, from Pioneer 10/11, Galileo, and Ulysses Data, of an Apparent Anomalous, Weak, Long-Range Acceleration," *Physical Review Letters*, Vol. 83, 1999, p. 1892; also http://arxiv.org/abs/gr-qc/9809070.

[9]Murphy, E. M., "A Prosaic Explanation for the Anomalous Accelerations Seen in Distant Spacecraft," *Physical Review Letters*, Vol. 83, 1999, p. 1890; also http://arxiv.org/abs/gr-qc/9810015.

[10]Scheffer, L. K., "Support for a Prosaic Explanation for the Anomalous Acceleration of Pioneer 10 and 11," 2001, http://arxiv.org/abs/gr-qc/0106010.

[11]Scheffer, L. K., "Conventional Forces Can Explain the Anomalous Acceleration of Pioneer 10," *Physical Review*, Vol. D67, 2003, pp. 084021-1–084021-11; also http://arxiv.org/abs/gr-qc/0107092.

[12]Scheffer, L. K., "A Conventional Physics Explanation for the Anomalous Acceleration of Pioneer 10/11," 2001, http://arxiv.org/abs/gr-qc/0108054.

[13]Anderson, J. D., Laing, P. A., Lau, E. L., Nieto, M. M., and Turyshev, S. G., "The Search for a Standard Explanation of the Pioneer Anomaly," *Modern Physics Letters*, Vol. A17, 2002, pp. 875–886; also http://arxiv.org/abs/gr-qc/0107022.

[14]Anderson, J. D. and Mashhoon, B., "Pioneer anomaly and the Helicity-Rotation Coupling," *Physics Letters*, Vol. A315, 2003, pp. 199–202; also http://arxiv.org/abs/gr-qc/0306024.

[15]Mashhoon, B., "Modification of the Doppler Effect Due to the Helicity–Rotation Coupling," *Physics Letters*, Vol. A306, 2002, pp. 66–72; also http://arxiv.org/abs/gr-qc/0209079.

[16]Hauck, J. C., and Mashhoon, B., "Electromagnetic Waves in a Rotating Frame of Reference," *Annalen der Physik*, Vol. 12, 2003, pp. 275–288; also http://arxiv.org/abs/gr-qc/0304069.

[17]Montenbruck, O., and Gill, E., *Satellite Orbits : Models, Methods, and Applications*, Springer-Verlag, Berlin, 2000.

[18]Talmadge, C., Berthias, J. P., Hellings, R. W., and Standish, E. M., "Model Independent Constraints on Possible Modifications of Newtonian Gravity," *Physical Review Letters*, Vol. 61, 1988, pp. 1159–1162.

[19]Anderson, J. D., Lau, E. L., Krisher, T. P., Dicus, D. A., Rosenbaum, D. C., and Teplitz, V. L., "Improved Bounds on Nonluminous Matter in Solar Orbit," *Astrophysical Journal*, Vol. 448, 1995, pp. 885–892; also http://arxiv.org/abs/hep-ph/9503368.

[20]Reynaud, S., and Jaekel, M.-T., "Testing the Newton Law at Long Distances," 2005, http://arxiv.org/abs/gr-qc/0501038.

[21]Eidelman, S., et al., "Review of Particle Physics," *Physics Letters*, Vol. B592, 2004, pp. 1–1109.

[22]Rosales, J. L., and Sanchez-Gomez, J. L., "A Possible Cosmologigal Origin of the Indicated Anomalous Acceleration in Pioneer 10/11 Orbital Data Analysis," 1998.

[23]Rosales, J. L., "The Pioneer Effect: A Cosmological Foucault's Experiment," 2002, http://arxiv.org/abs/gr-qc/0212019.

[24]Rosales, J. L., "The Pioneer's Anomalous Doppler Drift as a Berry Phase," 2004, http://arxiv.org/abs/gr-qc/0401014.

[25]Rosales, J. L., "The Pioneer Anomaly: The Measure of a Topological Phase Defect of Light in Cosmology," 2005.

[26]Ranada, A. F., "The Light Speed and the Interplay of the Quantum Vacuum, the Gravitation of All the Universe and the Fourth Heisenberg Relation," *International Journal of Modern Physics*, Vol. D12, 2003, pp. 1755–1762.
[27]Ranada, A. F., "The Pioneer Anomaly as Acceleration of the Clocks," *Foundations of Physics*, Vol. 34, 2005, pp. 1955–1971.
[28]Modanese, G., "Effect of a Scale-Dependent Cosmological Term on the Motion of Small Test Particles in a Schwarzschild Background," *Nuclear Physics*, Vol. B556, 1999, pp. 397–408; also http://arxiv.org/abs/gr-qc/9903085.
[29]Nottale, L., "The Pioneer Anomalous Acceleration: A Measurement of the Cosmological Constant at the Scale of the Solar System," 2003, http://arxiv.org/abs/gr-qc/0307042.
[30]Einstein, A., and Straus, E. G., "The Influence of the Expansion of Space on the Gravitation Fields Surrounding the Individual Stars," *Reviews of Modern Physics*, Vol. 17, No. 2-3, 1945, pp. 120–124.
[31]Cooperstock, F. I., Faraoni, V., and Vollick, D. N., "The Influence of the Cosmological Expansion on Local Systems," *Astrophysical Journal*, Vol. 503, 1998, pp. 61–66; also http://arxiv.org/abs/astro-ph/9803097.
[32]Milgrom, M., "A Modification of the Newtonian Dynamics as a Possible Alternative to the Hidden Mass Hypothesis," *Astrophysical Journal*, Vol. 270, 1983, pp. 365–370.
[33]Sanders, R. H., and McGaugh, S. S., "Modified Newtonian Dynamics as an Alternative to Dark Matter," *Annual Review of Astronomy and Astrophysics*, Vol. 40, 2002, pp. 263–317; also http://arxiv.org/abs/astro-ph/0204521.
[34]Bekenstein, J. D., "Relativistic Gravitation Theory for the MOND Paradigm," *Physical Review*, Vol. D70, 2004, pp. 083509-1–083509-1-28; also http://arxiv.org/abs/astro-ph/0403694.
[35]Moffat, J. W., "Modified Gravitational Theory and the Pioneer 10 and 11 Spacecraft Anomalous Acceleration," 2004, http://arxiv.org/abs/gr-qc/0405076.
[36]Milgrom, M., "MOND–Theoretical Aspects," *New Astronomical Review*, Vol. 46, 2002, pp. 741–753; also http://arxiv.org/abs/astro-ph/0207231.
[37]Jaekel, M.-T., and Reynaud, S., "Gravity Tests in the Solar System and the Pioneer Anomaly," *Mod. Phys. Lett.*, Vol. A20, 2005, p. 1047; also http://arxiv.org/abs/gr-qc/0410148.
[38]Jaekel, M.-T. and Reynaud, S., "Post-Einsteinian Tests of Linearized Gravitation," *Class. Quant. Grav.*, Vol. 22, 2005, pp. 2135–2158; also http://arxiv.org/abs/gr-qc/0502007.
[39]Barvinsky, A. O., Kamenshchik, A. Y., Rathke, A., and Kiefer, C., "Braneworld Effective Action: An Alternative to Kaluza–Klein Reduction," *Physical Review*, Vol. D67, 2003, pp. 023513-1–023513-19; also http://arxiv.org/abs/hep-th/0206188.
[40]Barvinsky, A. O., "Nonlocal Action for Long-Distance Modifications of Gravity Theory," *Physics Letters*, Vol. B572, 2003, pp. 109–116; also http://arxiv.org/abs/hep-th/0304229.
[41]Smilga, A. V., "Benign vs. Malicious Ghosts in Higher-Derivative Theories," *Nuclear Physics*, Vol. B706, 2005, pp. 598–614; also http://arxiv.org/abs/hep-th/0407231.
[42]Bertolami, O., and Paramos, J., "The Pioneer Anomaly in a Bimetric Theory of Gravity on the Brane," *Classical and Quantum Gravity*, Vol. 21, 2004, pp. 3309–3321; also http://arxiv.org/abs/gr-qc/0310101.
[43]Defrère, D., and Rathke, A., "Pioneer Anomaly: What Can We Learn from LISA?," 2005, http://arxiv.org/abs/gr-qc/0509021.
[44]Tsuyuki, G. T., and Mireles, V., "A Summary of the Cassini System-Level Thermal Balance Test: Engineering Subsystems," http://hdl.handle.net/2014/22130.
[45]Verdant, M., and Schwehm, G. H., "The International Rosetta Mission," *ESA Bulletin*, Vol. 93, Feb. 2002, pp. 12–24.
[46]Stern, A., and Spencer, J., "New Horizons: The First Reconnaissance Mission to Bodies in the Kuiper Belt," *Earth, Moon and Planets*, Vol. 92, 2003, pp. 477–482.
[47]Bertolami, O., and Tajmar, M., "Gravity Control and Possible Influence on Space Propulsion," Technical Rept. CR(P)4365, ESA, 2002.
[48]Anderson, J. D., Nieto, M. M., and Turyshev, S. G., "A Mission to Test the Pioneer Anomaly," *International Journal of Modern Physics*, Vol. D11, 2002, pp. 1545–1552; also http://arxiv.org/abs/gr-qc/0205059.
[49]Dittus, H. et al., "A mission to Explore the Pioneer Anomaly," *39th ESLAB Symposium: Trends in Space Science and Cosmic Vision 2020*, April 2005, http://arxiv.org/abs/gr-qc/ 0506139.
[50]Johann, U., and Förstner, R., "A Small Mission to Explore the Pioneer Anomaly and Potentially to Discover Local Evidence for Dark Matter or Dark Energy," unsolicited mission proposal to ESA, Oct. 2003.
[51]Penanen, K., and Chui, T., "A Novel Two-Step Laser Ranging Technique for a Precision Test of the Theory of Gravity," *Nuclear Physics Proceedings Supplement*, Vol. 134, 2004, pp. 211–213; also http://arxiv.org/abs/gr-qc/0406013.
[52]Bondo, T., Walker, R., Willig, A., Rathke, A., Izzo, D., and Ayre, M., "Preliminary Design of an Advanced Mission to Pluto," 24th International Symposium on Space Technology and Science, Paper, ISTS 2004-r-49, June 2004.
[53]Rathke, A., "Testing for the Pioneer Anomaly on a Pluto Exploration Mission," *International Work-shop on Frontier Science: Physics and Astrophysics in Space*, June 2004; also http://arxiv.org/abs/astroph/ 0409373.
[54]Vasile, M., Summerer, L., Linder, N., Saive, G., and Silvestri, C., "Advanced Trajectory Options for the Exploration of the Outer Solar System," 24th International Symposium on Space Technology and Science, Paper ISTS 2004-k-10, June 2004.
[55]Izzo, D., Bevilacqua, R., and Valente, C., "Optimal Large Reorientation Manoeuver of a Spinning Gyrostat," *6th Cranfield Conference on Dynamics and Control of Systems and Structures in Space: 2004*, 2004, pp. 607–616.
[56]Lyngvi, A., Falkner, P., Kemble, S., Leipold, M., and Peacock, A., "The Interstellar Heliopause Probe," 55th International Astronautical Congress, Paper IAC-04-Q.2.A.06, Oct. 2004.
[57]Longuski, J., Todd, R., and König, W., "A Survey of Nongravitational Forces and Space Environmental Torques with Applications to the Galileo Spacecraft," *Journal of Guidance and Control*, Vol. 15, No. 3, 1982, pp. 545–553.
[58]Cruikshank, D. P., "Yarkovsky and His Effect," *Bulletin of the American Astronomical Society*, Vol. 9, June 1977, p. 458.
[59]Peterson, C., "A Major Perturbing Force on Small ($1 < R < 10^4$ cm) Solar System Bodies; The Yarkovsky Effect," *Bulletin of the American Astronomical Society*, Vol. 7, March 1975, p. 376.
[60]Van der Ha, J., and Modi, V., "Analytical Evaluation of Solar Radiation Induced Orbital Perturbations of Space Structures," *Journal of the Astronautical Sciences*, Vol. 25, 1977, pp. 283–306.
[61]Mui, D., and Allasio, A., "GOCE: The First Core Earth Explorer of ESA's Earth Observation Programme," *Acta Astronautica*, Vol. 54, 2003, pp. 167–175.
[62]Thornton, C. L., and Border, J. S., "Radiometric Tracking Techniques for Deep-Space Navigation," Deep-Space Communications and Navigation Series 00-11," Jet Propulsion Lab., Pasadena, CA, 2000.
[63]Kinman, P. W., "Doppler Tracking of Planetary Spacecraft," *IEEE Transactions on Microwave Theory and Techniques*, Vol. 40, 1992, pp. 1199–1204.
[64]Melbourne, W. G., and Curkendall, D. W., "Radio Metric Direction Finding: A New Approach to Deep Space Navigation," AIAA/American Astronautical Society Astrodynamics Specialist Conf., Sept. 1977.
[65]Jones, D. L., "Spacecraft Tracking with the SKA," *Science with the Square Kilometer Array New Astronomy Reviews*, 2004; also http://arxiv.org/abs/astro-ph/0409354.
[66]Bate, R. R., White, J. E., and Mueller, D., *Fundamentals of Astrodynamics*, Dover, New York, 1971.
[67]Curkendall, D. W., and McReynolds, S. R., "A Simplified Approach for Determining the Information Content of Radio Tracking Data," *Journal of Spacecraft and Rockets*, Vol. 6, 1969, pp. 520–525.
[68]Nieto, M. M., "Analytic Gravitational-Force Calculations for Models of the Kuiper Belt," 2005; also http://arxiv.org/abs/astro-ph/0506281.
[69]Vasile, M., Bisbroek, R., Summerer, L., Galvez, A., and Kminek, G., "Options for a Mission to Pluto and Beyond," American Astronautical Society, Paper AAS 03-210, 2003.
[70]Izzo, D., Markot, M. C., and Nann, I., "A Distributed Global Optimizer Applied to the Design of a Constellation Performing Radio-Occultation Measurements," AAS/AIAA Space Flight Mechanics Conf., American Astronautical Society, Paper AAS 05-150, Jan. 2005.
[71]Storn, R., and Price, K., "Differential Evolution—A Simple Efficient Heuristic for Global Optimisation over Continuous Space," *Journal of Global Optimisation*, Vol. 11, 1997, pp. 341–359.
[72]Gobetz, F. W., "Optimal Transfers Between Hyperbolic Asymptotes," *AIAA Journal*, Vol. 1, No. 9, 1963, pp. 2034–2041.

D. Spencer
Associate Editor